

Report of Committee V.1
12th Int. Ship and Offshore Structures Congress 1994
St. John's, Newfoundland, Canada

APPLIED DESIGN – STRENGTH LIMIT STATES FORMULATIONS

Concern for the applicability of formulations related to the ultimate, buckling and the fatigue strength of structural components of ships, offshore platforms, and other marine structures. Emphasis shall be given to comparisons with available experimental data compiled in terms of probabilistic measures to evaluate the accuracy of these formulations for use in reliability-based design procedures.

<i>CHAIRMAN:</i>	Prof. T. Moan
<i>MEMBERS:</i>	Dr. P. A. Frieze
	Prof. C. Ganapathy
	Dr. T. Hori
	Prof. A. E. Mansour
	Mr. G. Parmentier
	Dr. P. H. Rigo
	Dr. V. Zanic

CONTENTS

1. INTRODUCTION
2. LIMIT STATES AND UNCERTAINTY MODELLING
 - 2.1 Limit state formats
 - 2.2 Model uncertainty
 - 2.3 Model, parameter and total uncertainty
 - 2.4 Characteristic and design values of resistance
3. ULTIMATE LIMIT STATES FOR STEEL-PLATED COMPONENTS
 - 3.1 Introduction
 - 3.2 Plate elements
 - 3.2.1 Formulations
 - 3.2.2 Uncertainty measures
 - 3.3 Stiffened panels subject to axial compression
 - 3.3.1 Formulations
 - 3.3.2 Uncertainty measures
 - 3.4 Stiffened panels subject to axial compression and bending or lateral pressure
 - 3.4.1 Formulations
 - 3.4.2 Uncertainty measures
 - 3.5 Benchmark test of stiffened panels
 - 3.6 Stiffened girders subject to in-plane axial and bending stresses
 - 3.6.1 General
 - 3.6.2 Plate failure modes
 - 3.6.3 Overall failure of narrow girder flanges and stiffeners
 - 3.6.4 Uncertainty measures
 - 3.7 Girders under predominantly in-plane shear stresses
 - 3.7.1 General
 - 3.7.2 Effect of direct and bending stresses - interaction between shear and bending
 - 3.7.3 Stiffener requirements
 - 3.7.4 Effect of web cut-outs
 - 3.7.5 Uncertainty measures
4. ULTIMATE LIMIT STATES FOR CYLINDRICAL SHELLS
 - 4.1 Introduction
 - 4.2 Overall column and beam-column collapse
 - 4.2.1 Failure modes and formulations
 - 4.2.2 Column capacity
 - 4.2.3 Bending
 - 4.2.4 Axial compression and bending
 - 4.2.5 Axial compression, bending and hoop compression
 - 4.2.6 Uncertainty measures
 - 4.3 Local buckling of unstiffened and ring stiffened shells
 - 4.3.1 Failure modes
 - 4.3.2 Axial compression and bending
 - 4.3.3 Hoop compression
 - 4.3.4 Axial loading and hoop compression
 - 4.3.5 Uncertainty measures

- 4.4 Frames in ring stiffened cylinders
- 4.5 Orthogonally stiffened shells
 - 4.5.1 Failure modes and formulations
 - 4.5.2 Axial loading
 - 4.5.3 Radial loading
 - 4.5.4 Combined axial and radial loading
 - 4.5.5 Uncertainty measures

- 5. ULTIMATE STRENGTH OF TUBULAR JOINTS
 - 5.1 General
 - 5.2 Formulations for simple joints
 - 5.3 Model uncertainty for simple joints
 - 5.4 Other joints

- 6. FATIGUE LIMIT STATES FOR WELDED JOINTS
 - 6.1 General
 - 6.2 SN curves and stress concentration
 - 6.3 Model uncertainties
 - 6.3.1 General
 - 6.3.2 Stress concentration factors
 - 6.3.3 Miner Palmgren hypothesis

- 7. CONCLUSIONS

ACKNOWLEDGEMENT

REFERENCES

1. INTRODUCTION

Marine structures are designed to fulfill serviceability (SLS) and ultimate limit state (ULS) criteria. The latter category in general comprises criteria for structural integrity, and may be further classified in terms of /1/:

- ultimate limit state of components
- ultimate limit state of systems
- fatigue limit state of components

The ultimate limit may be characterized by loss of equilibrium, fracture or excessive deformation. The fatigue limit state is defined by a crack size that represents an ultimate limit /1, 2/.

Marine metal structures are made of beams, stiffened panels, shells, and joints. Ultimate limit states may be expressed by parametric formula, numerical calculation procedures (e.g., nonlinear finite elements), or by testing. Existing component ultimate limit states are generally given by parametric formulae in terms of stresses, forces or moments; and exceptionally by strains, which have been justified by test results. Fatigue criteria in design codes are typically expressed by SN curves. Numerical approaches usually need to be used in connection with systems capacity. Design by testing (alone) may be used in special cases of innovative design.

There are significant differences between formulae used in different codes for the same failure mode. Hence, there is a need to compare and harmonize strength expressions, to identify the "best" one. Efforts to harmonize requirements for ships are made through IACS; and for offshore structures through ISO. There is a need to harmonize ship and offshore strength requirements, especially for steel-plated components.

The purpose of this report is to review ultimate and fatigue limit states for steel components in marine structures. The focus is on formulations of beam-columns, stiffened plates and shells and planar and tubular joints given in terms of parametric equations. Approaches specified as a numerical procedure will be briefly commented upon, in cases where they seem to offer significant improvement compared to parametric formulae.

The mathematical expressions for the limit states will be used as a basis for:

- failure function for reliability analysis. In this case the parameters in the limit state are considered to be random variables.
- design equations. In this case the parameters in the limit state - according to the partial factor method - are given by their characteristic values, each multiplied by a partial safety factor.

However, for a given phenomenon, the same limit state formulation may not necessarily be applied for the design equation and the failure function; but a more optimal calibration is achieved by choosing the same limit state.

A particular issue of concern in connection with buoy marine structures is the definition of ultimate limit state view of conditions where large deformations/strains cause failure/fracture and, hence, possible leakage. "Wet tightness" may in principle be considered as a separate limit state, which may imply a lower limit on deformations dictated by the pure load carrying capacity.

Generally, several formulations are applied for different limit states. Significant efforts would be required to compare existing formulations to establish the "best" approach. The committee has attempted to collect available information on selected failure modes that could be considered as a model contribution to future efforts of improving the corresponding limit states.

Clearly, existing codes for marine and civil engineering structures should form the basis for the assessment of limit states. Recent systematic experimental or numerical analyses as reviewed by other ISSC committees, are useful as a basis for code modification. Due to space limitation, only selected references can be quoted by this committee.

Ship rules have traditionally represented prescriptive criteria for scantlings, which reflect strength and fatigue and other considerations. So-called direct calculation methods for ships are usually based on explicit loads and stress formulae. However, these formulations are often based on linear yielding and elastic buckling with a simple correction for plasticity, i.e., not truly ultimate limit states. For lack of space, such methods will only briefly be touched upon here. On the other hand, explicit fatigue criteria that have recently been introduced for ships, are considered.

The current availability of accurate numerical methods allows determination of the strength on a case basis as well as to accomplish systematic studies of complex structures. A particular advantage of numerical methods is that the effect of each factor can be studied separately. However, numerical methods to trace nonlinear behavior up to collapse are susceptible to various sources of uncertainty, including human errors of different kinds. It is, therefore, necessary to standardize the relevant numerical analysis procedures. It may even be necessary to "certify users" and validate results before such analyses can be used by designers at large to determine resistances.

Up to now, ultimate strength formulations in codes have been established primarily on the basis of simple structural mechanics models, with appropriate "knock down" factors determined experimentally. Relatively simple and accurate formulations are achievable when failure mode follows a simple mechanism (buckling, yield hinge mechanism, etc.).

achieve such simple failure modes, e.g., for complex stiffened, thin walled plates and shells, the stiffeners are considered to meet certain assumptions, which commonly are conservative.

This review refers to "strength of materials" type design formulations supported by experiments or systematic numerical studies. The main source of information for the limit states of concern herein are codes issued by the industry, governmental regulatory bodies and classification societies. Review of recent developments of analytical and numerical techniques as well as experimental methods as such, is outside the scope of this report. The aim is rather to address some possible directions of further code developments. To come up with a new code, is certainly beyond the scope of this ISSC committee.

Chapter 2 deals with various formats for limit states and a consistent assessment of the inherent uncertainties.

Chapters 3-6 present comparisons between limit states used for the different types of components.

A summary and recommendations for future work are given in Chapter 7.

2 LIMIT STATES AND UNCERTAINTY MODELLING

2.1 Limit state formats

Limit states should /6,7/:

- preferably be based on structural mechanics theoretical formulations (not pure regression to data)
- explicitly contain the parameters of influence
- have as small (random) model uncertainty as possible
- be as simple as possible

Limit states should, as far as possible, be based on the strength of materials, elastic buckling formulae, plastic limit loads, etc., appropriately modified to account for residual stresses and geometrical imperfections, and should be obtained by a pure regression analysis of test results. It would also be advantageous that a formulation converges for slender and stocky components, respectively. Besides nominal dimensions of the components, the stress-strain curve, geometrical imperfections and residual stresses are parameters of influence. Only the yield stress, and not the stress-strain curve, is commonly referred to in resistance formulations. Maximum geometrical deviations are usually assumed when developing the strength limit states; and tolerance requirements are imposed in design to ensure that they are complied with during fabrication. The residual stress pattern depends upon the fabrication, and is generally not explicitly accounted for.

Limit states are subject to a systematic and random uncertainty. As discussed below, the systematic component is accounted for directly, while the random component implies a partial safety (material) factor.

Simplicity in the design formulation implies a reduced chance of gross errors.

2.2 Model uncertainty

For a structural component subject to one load (i.e., plane compression, or lateral pressure), s_1 at a time, the predicted resistance, $r_{pred,i}(z)$ is a function of a set of variables, which may include yield strength, plate thickness, geometrical imperfection, etc. Usually these parameters vary over the component, and each type of parameter is represented by its value at a few locations, assuming that the variation follows some pattern over the structure. Typical out-of-plane imperfections may be described by Fourier components /3/. The yield stress is different in different directions, and in compression versus tension, and depends on strain rate. It is important that the model uncertainty be assessed using the same definition of yield stress as used

design analyses. The resistance model is uncertain. By characterizing this model uncertainty by Δ_i , the actual resistance, $r_{\text{true},i}$ corresponding to a load s_i , may be written as /4/:

$$r_{\text{true},i} = \Delta_i r_{\text{pred},i}(z) \quad (1)$$

The model uncertainty, Δ_i is assessed by comparing predictions with results obtained by experiments or advanced numerical analyses, most often by assuming that the error in experimental or numerical calculations is negligible. The predictions are made by using a representative value of the parameters in the set, z_j corresponding to the specimen no. j . The corresponding sample of Δ_i is:

$$\Delta_i^{(j)} = r_{(\text{test})}^{(j)} / r_{(\text{pred})}^{(j)}(z_j) \quad (2)$$

The statistics of Δ_i may then be calculated based on a sample $\{\Delta_i^{(j)}\}$. Usually limited information is available, and Δ_i is simply modelled by a normal or lognormal distribution.

In some cases, it may be interesting to determine the model uncertainty Δ_i as a function of some (geometrical or other) parameters. Hence, the uncertainty for beam-columns may firstly be determined for each type of member cross-section. Secondly, for a given type of component under compressive stresses, it may be convenient to determine Δ_i , as a function of slenderness, because the uncertainty will depend upon whether it is buckling or plastic collapse that leads the component to reach its ultimate limit state. Such information may be useful in the first place to assess whether a trend in the bias may warrant a modified strength formulation, and secondly whether the partial safety factor should depend upon this parameter (e.g., slenderness).

It follows from the above assumptions, that before applying experimental or numerical data to assess the uncertainty, they should be critically reviewed to eliminate data influenced by "gross" errors, or experimental data which involve incompletely defined tests. This is a major task in an uncertainty assessment.

Model uncertainties for the ultimate strength of components which are subject to two or more load components also need to be described. In general, the interaction equation may be written as:

$$g\left(\left\{\frac{s_i}{r_i}\right\}, \{c_k\}\right) = 0 \quad (3)$$

where s_i and r_i are load effects and resistances corresponding to load component no. (i), $\{c_k\}$ is a set of coefficients used

in the model. The interaction for the case of two loads illustrated in Fig. 1.

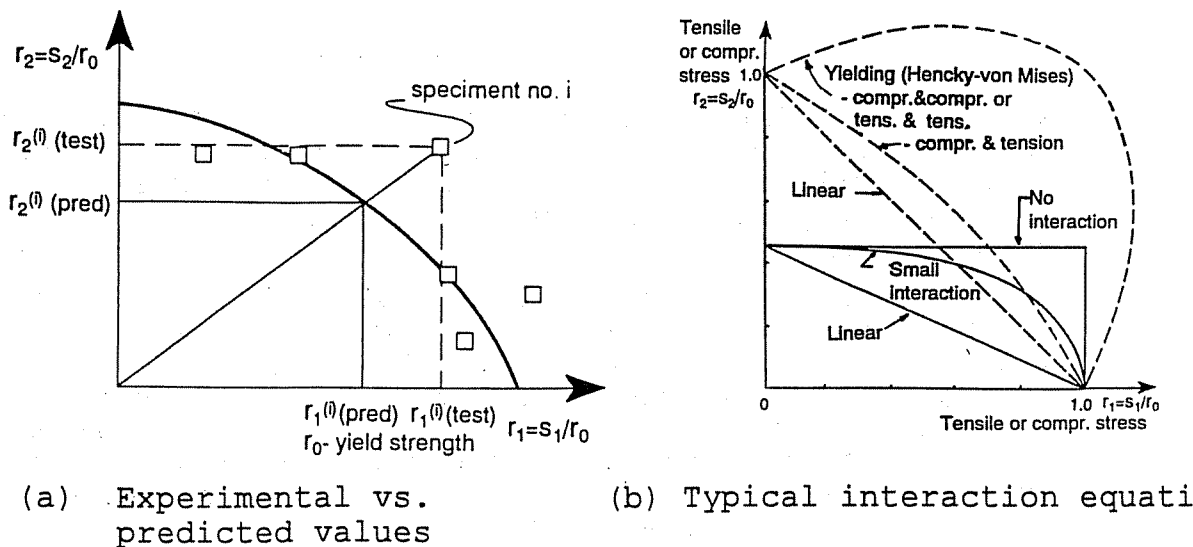


Fig. 1 Strength interaction for two action effects

The model uncertainty of the interaction equation should be expressed so that it represents the model uncertainty each basic load case as a special case when only one load, is acting. This means that each r_i should be modified with which is determined for each r_i as explained above. In addition, uncertainties, Δ_k need to be associated with other parameters, $\{c_k\}$ in the interaction formula, Eq. (4), e.g.:

$$g(\{s_i/\Delta_i r_i\}, \{\Delta_k c_k\}) = 0$$

If, for instance, the basic interaction equation consists of terms like $(s_i/r_i)^{\alpha_i}$, terms of the type:

$$\Delta_k c_k (s_i/r_i)^{\alpha_i} (s_j/r_j)^{\alpha_j}$$

may be introduced to account for uncertainties of interaction. A convenient way to characterize the uncertainty for the case of two loads (Fig. 1a) is by:

$$\Delta_{12}^{(j)} = r_{1(test)}^{(j)} / r_{1(pred)}^{(j)} = r_{2(test)}^{(j)} / r_{2(pred)}^{(j)} \quad (4)$$

where $r_{i(test)}^{(j)}$ is the experimental resistance corresponding to the load i . Then, it needs to be demonstrated by a certain choice of Δ_k , that Eq. (4) implies the same uncertainty expressed by $\Delta_{12} / 7/$. If the discrepancy is unacceptable, improved interaction equation should be introduced.

If, however, interaction between, e.g., two loads s_1 and s_2 is considered, the interaction of the load

limited to the range 0 to \bar{s}_2/r_2 , the interaction equation may be expressed in terms of s_1/r_1 , and the model uncertainty, Δ_1 may be calculated by:

$$\Delta_1 = r_{1(\text{test})}^{(j)} / r_{1(\text{pred})}^{(j)} \quad (5b)$$

In this case (all) the uncertainty Δ_1 should be assigned to the variable r_1 , also for the case when $s_2 > 0$. Clearly, this approach will not be particularly accurate when s_2 varies from 0 to r_2 , which implies a variation between a pure s_1 and a pure s_2 load condition.

An analogous interaction problem exists for fatigue, both in relation to crack initiation and crack growth, under multiaxial stress conditions. While the equivalent (plastic) strain would be a representative measure for crack initiation, tensile stresses normal to crack and shear stresses are the relevant stresses for crack growth. However, the normal stress usually dominates and the shear contribution is rarely considered for marine structures.

2.3 Model, parameter and total uncertainty

The resistance is influenced, for instance, by overall scantlings (a, b, \dots), plate thickness (t), initial imperfection (δ), modulus of elasticity (E), yield stress (σ_0) and residual stress (σ_r). Representative values of the parameters a , t , and σ_0 are commonly explicitly accounted for in ultimate resistance formulae. Values of initial imperfections and residual stresses are often only implicitly assumed when establishing the resistance formula. Imperfections (δ) are, however, controlled by tolerance requirements. Residual stresses, σ_r are treated explicitly, e.g., in connection with stiffened cylinders.

When, for instance, initial imperfections are not explicitly considered in $r_{\text{pred}}(z)$, and the variation of imperfections in real structural components is not the same as in the test specimens used to estimate Δ_1 , the model uncertainty Δ_1 needs to be modified to be considered representative for real components, /7/.

If the sample of specimens used to determine Δ_1 , is small, the statistical uncertainty should be combined with the model uncertainty using Bayesian methods /5/.

However, in some cases, the experimental/numerical data basis is applied in the first place to fit the theoretical model to the data. In that case, the model uncertainty Δ_1 determined by the above procedure, obviously does not reflect the true model uncertainty, and Δ_1 needs to be (subjectively) adjusted.

Finally, the relevance of the material, geometry and boundary as well as load conditions used in the experimental/numerical investigation to determine the model

necessary to modify Δ_i for a particular application of prediction method, r_{pred} .

2.4 Characteristic and design values of resistance

Uncertainties should be handled by probabilistic methods. If a simple design criterion in terms of a single resistance R_i and load effect, S_i is considered, and, e.g., a lognormal probability distribution is assumed for R_i and S_i , the design values of R_i and S_i can be separated, and the design value r_i becomes /1/:

$$r_{id} \cong \mu_{r_i} \exp[-\alpha_{r_i} \cdot \beta_T \cdot V_{r_i}]$$

where μ_{r_i} and V_{r_i} are the mean and COV of R_i , respectively, and β_T are the so-called sensitivity factors and the target reliability index, respectively. α_{r_i} depends upon the relative magnitude of the uncertainties in R_i and S_i , and, varies between 0.2 and 1.0. α_{r_i} will typically be smaller for slender members in bottom supported platforms subjected to wave loads than for panel and shell components in large volume marine structures, or structures subjected predominantly to hydrostatic pressure, because of the relative magnitude of load and resistance uncertainties. In the design value method which yields a simplified code calibration, α_{r_i} is taken to be 0.8.

The characteristic value for a lognormal variable, R_i can be defined by means of μ_{r_i} and V_{r_i} as:

$$r_{ik} \cong \mu_{r_i} \exp[-k_{r_i} V_{r_i}] \quad \text{for } V_{r_i} \leq 0.2$$

where k_{r_i} is a constant which is selected so that r_{ik} is defined according to a certain fractile value, and is typically of the order 0.5 to 1.5.

The partial resistance factor, γ_{Ri} may be defined by:

$$\gamma_{Ri} = \frac{r_{ik}}{r_{id}} \cong \exp[(\alpha_{r_i} \beta_T - k_{r_i}) V_{r_i}]$$

Hence, with $k_{r_i} = 1.5$, $\alpha_{r_i} = 0.5$ and a target safety factor corresponding to $\beta_T = 4.2$, $\gamma_{Ri} \sim 1 + 0.6V_{r_i}$.

Eq. (8) applies if the design resistance r_{id} is based on Eq. (1), e.g., corrected due to Δ_i . If the design is based on r_{pred} , the safety factor to achieve a target reliability would be γ_{Ri}/μ_{Δ} , where μ_{Δ} is the mean Δ_i . This shows the important influence of the bias in the resistance.

3. ULTIMATE LIMIT STATES FOR STEEL-PLATED COMPONENTS

3.1 Introduction

Basically two main types of steel-plated components are applied in marine structures (Fig. 2):

- stiffened panels subjected to predominantly in-plane axial stresses, but with some in-plane transverse and shear stresses and possibly lateral pressure
- stiffened girders subjected primarily to in-plane shear and longitudinal axial and bending stresses

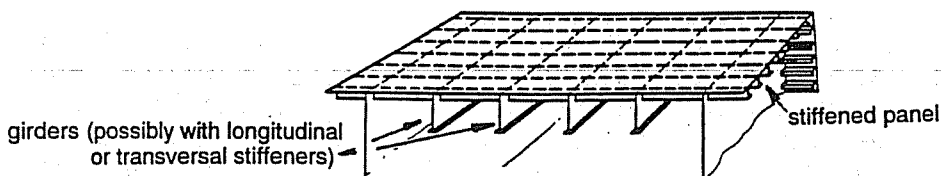


Fig. 2 Stiffened panels/girders

The collapse behavior of stiffened panels and girders received considerable attention in the 1970's and 1980's, especially in connection with several box girder bridge failures, culminating in the codes such as BS 5400 /9/ and EC3/ECCS /13,14/. Much of this work has been focused on modern limit state methods.

While the civil engineering developments of ultimate limit states for stiffened panels for bridges had some influence on marine practice, the significant efforts on stiffened girders in bridges have so far had less effect on the design practice for similar components in marine practice.

The disadvantage with EC3/ECCS, BS5400 and other codes primarily developed for civil engineering structures is that they do not cover geometries and load conditions (e.g., in-plane and lateral pressure) typical of marine structures. Ship rules of classification societies are based on elastic/plastic buckling/first yield criteria, but since the formulations are implicit in scantling requirements, they are not pursued herein. Especially, the involvement of some classification societies in structures for offshore oil exploitation, which initially was heavily influenced by civil engineering practice, has made them introduce limit state formulations. Det norske Veritas has introduced a comprehensive guidance /11/, while Bureau Veritas /10/, Germanischer Lloyd (GL) /15/ and other societies follow. GL, for instance, base their recent (offshore) codes on Eurocode 3 (ECCS) and DIN 18800. Besides classification societies, governmental regulatory bodies such as HSE /16/ and NPD /17/ in the UK and Norway, respectively; and API (in the USA) issue codes for offshore structures.

Recent state-of-the-art reports on steel-plated structures /18-21/ refer primarily to civil engineering components, are partly relevant to marine structures.

However, the research goes on in this area, as reported by the ISSC Committee III.1, generally by using experimental and numerical methods. In this report, the focus will be on using data obtained by systematic numerical or experimental studies to validate strength codes based on parametric formulae. Some publications deal with the uncertainties in the strength. For this reason, this committee launched a benchmark study; /22/ and the brief summary in Section 3.5. The benchmark study was also done to assess the robustness of the formulations and calculations, with respect to human errors.

Stiffened panels may exhibit the following failure modes depending upon the geometry and material property:

- local buckling or collapse of plate between stiffeners
- local buckling or collapse of stiffeners. The basic design philosophy is to avoid such failure modes by slenderness requirements
- overall buckling of stiffened panel between frames and bulkheads

Limit states for the first failure mode are discussed in Section 3.2. Overall collapse of stiffened panels under axial and possible lateral loads (bending moments) is treated in Sections 3.3 and 3.4, while the benchmark test for such panels is described in Section 3.5. The overall collapse of stiffened girders subjected to in-plane bending and shear is discussed in Sections 3.6 and 3.7.

3.2 Plate elements

3.2.1 Formulations

The basic component is a plate element subjected to axial or lateral loads.

In modern limit state approaches the design principle is to assume that the plate element reaches its collapse load before overall stiffener failure. Estimates of the ultimate limit capacity of plate elements are therefore crucial.

Significant efforts have been devoted to improving the original Von Karman estimate of the ultimate strength of an axially loaded plate. Various in-plane and flexural boundary conditions, and imperfections and residual stresses need to be considered. Recent reviews of the various formulations have been made in /18,23-29/. Some of the discrepancies between different specifications may be explained by different assumptions regarding initial imperfection, boundary conditions and residual stress levels, which are all factors of influence.

In particular, it is noted that the different codes specify different level of acceptable imperfection tolerance!

For instance, the tolerance requirement for initial imperfection of plating varies, and the imperfection amplitude to plate width is, e.g., $w_0/b < 0.01$ (API Bul. 2V /8/, DnV /11/, 1987), $w_0/b \leq 0.002$ (ECCS /13/). According to BS 5400 /9/, it varies with a/b and σ_0 , but is approximately $w_0/b \leq 0.01$. The allowable initial deflection of stiffeners is in the range 1/750 of the span (BS 5400) to 1/500 (ECCS). Considering moderate imperfections ($w/t = 0.1\beta^2$, where β is normalized plate slenderness) and compressive residual stresses ($0.15\sigma_0$), the following ultimate to yield strength, σ_u/σ_0 was proposed in /23,28/:

$$\sigma_u/\sigma_0 = 0.23 + 1.16/\beta - 0.48/\beta^2 + 0.09/\beta^3 \quad (9)$$

which slightly deviates from previously proposed formulae.

An assessment of the sensitivity of σ_u to imperfections is given in /26/. Experimental results are compared with numerical results using moderate imperfections ($w_0/t = 0.1\beta^2$) in real plates as well as numerical results using actual imperfections of the specimens; see Fig. 3. The effect of residual stresses and imperfections was also studied in /29,30/.

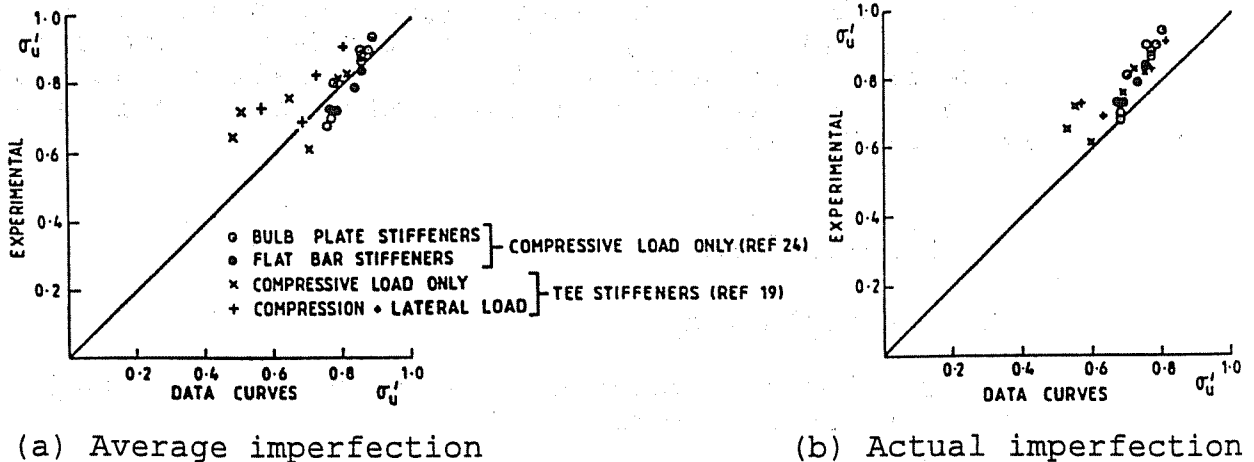


Fig. 3 Comparison of numerical and experimental results /20/. Numerical predictions using average or actual imperfection.

An interaction formula for biaxial compression was proposed in /24,27/, which converges to the von Mises-Hencky and linear interaction for stocky and very slender plates, respectively. Also, an interaction curve for biaxial compression and shear is given in /24,27/. Based on ultimate limit state formulation, it is concluded for the shear strength in /24/ that the DnV curves are rational, but generally

conservative and the LR rules are too simplistic and lead to varying levels if the same safety factor is applied.

A special phenomenon is observed for slender panels (e.g., $\beta \geq 3$) supported by strong stiffeners subjected to shear loading, in that a tension field is developed and, hence, leads to significant capacity beyond linear shear buckling (see Section 3.7).

Concerning lateral pressure combined with biaxial compression, interaction curves are provided in /25/ for particular imperfections and a range of aspect ratios, slenderness and pressures. These curves are translated into parametric formulations to give the variation of the strength with the lateral pressure. This model predicts that lateral pressure has a much greater effect on compressive resistance than suggested by current design rules.

3.2.2 Uncertainty measures

The uncertainty of predicted ultimate strength (effective width) of plating can be assessed based on the results displayed in Fig. 3 /26/. It is seen that the smallest safety factor defined according to Eq. (2) (of 1.05) is achieved when predictions are made on the basis of average imperfections. The scatter then corresponds to a COV of 13%. If the average imperfection is used, the bias surprisingly increases to 13% but the COV is reduced to 7%.

3.3 Stiffened panels subject to axial compression

3.3.1 Formulations

The strength of stiffened panels under axial compression may be treated as

- a series of disconnected beams
- an orthotropic plate
- a discretely stiffened plate

For most (wide) stiffened panels, the "column" approach considering flexural collapse of a single stiffener with adjacent plate, is adopted. Local buckling of the stiffener is avoided by assuming that their geometry fulfills certain local slenderness constraints. Generally, two different "column" approaches are applied. The first approach is based on reduced slenderness concept with a strength expressed in terms of the Euler buckling load, modified for elasto-plastic behavior by the Johnson-Ostenfeld parabola (API Bul. 2V, ship rules). The second method is the Perry approach (e.g. BS 5400, DnV, ECCS). Recently, various methods used for predicting the ultimate strength of stiffened panels (

axial compression) have been assessed and new methods proposed /31,32/.

The beam model is sometimes established by taking the plate flange to have a given effective width, while in others, the relative effective width is to taken to be the ultimate strength σ_u/σ_o , according to, e.g., Eq. (9) for axial compression. For tension flanges, the relative width is 1.0. The basic Perry equation for a column subjected to an axial compressive force P and a bending moment, M at a cross section with an effective area A_{eff} and an effective moment of inertia, I_{eff} is:

$$\frac{P}{A_{eff}} + \omega \frac{M}{I_{eff}} y = \frac{P_o}{A_{eff}} \quad (10)$$

where y is the distance from the neutral axis to the outer fiber, ω is ± 1 and P_o the yield load. For an imperfect column under axial compression, the maximum bending moment is approximately taken as:

$$M = \Delta_o \cdot P / (1 - P/P_E) \quad (11a)$$

where the Δ_o is the initial imperfection and P_E the Euler load.

In evaluating the collapse stress using the Perry equation, it is necessary to examine two cases as the overall column initial geometrical imperfection (Δ_o) may occur in a direction towards the plate or towards the stiffener tip. For each of these two cases, the check point (i.e., the value of y) may be different, depending on whether the stress check for compressive yield is applied to the plating (PC) or to the stiffener (SC).

To account for transverse or shear stresses in the plating, an efficient yield stress may be applied; see, e.g. DnV-CNB /11/.

In Eq. (10), $\omega = 1$ when checking against compressive failure either in the plate panel (PC) or at the stiffener tip (SC) while, on the other hand, $\omega = -1$ when checking against tensile failure at the stiffener tip (ST).

Eqs. (10-11a) may be readily solved and $\sigma_u = P_u/A_{eff}$ expressed in terms of Δ_o , ω , σ_o and $\sigma_E = P_E/A_{eff}$. Different codes specify different values of the "effective" imperfection parameter Δ_o . It is noted that the ECCS (column) approach is a modified "Perry approach" by referring to the stress at the cross-section centroid rather than the stiffener tip stress. DnV introduces an imperfection for the collapse mode associated with the column deflection towards the stiffener tip. However, it is pointed out in /30,31/ that in the analysis of continuous panels, the line of action of the load is allowed to follow this shift in neutral axis, and the correction is unnecessary.

The column approach does not normally cater for tripping of stiffeners. At present, it is usual to specify slenderness

criteria to prevent this mode from occurring prior to overall collapse. Some relaxation on the slenderness limitation is possible if the stiffener is not fully stressed or if the stress distribution across the depth has a high bending component. In most cases, these criteria are based on the buckling response of a single stiffener outstand, modeled as a plate panel under uniform axial compression with three edges simply supported and one edge free, but this model cannot properly take into account the interaction between the plate and the stiffener /34,35/. Plate buckling, which precedes the ultimate limit state, may initiate deformation and premature stiffener failure /35/. While this problem can be analyzed by numerical methods, appropriate "strength of materials design code formulations", are still lacking.

The strength of narrow stiffened flanges with only a few longitudinal stiffeners can be underestimated by the current approach, since transverse action may be significant. The ECCS provides a strength formulation for orthotropic stiffened panels.

3.3.2 Uncertainty measures

The uncertainty of existing code formulations (DnV, BS 5400, and API) and a method proposed by the research group at Imperial College has been assessed by using the results of 23 tests for axially compressed panels /31,32/. The imperfections and residual stresses in the prediction models are taken as fixed, not varied according to those in the specimens. The results are summarized in Table 1. The results are not included because this method does not seem to have been correctly used in /31/. It is seen that the bias and COV are almost the same (1.10 and 15%) for all methods, except that the proposed IC-method yields less scatter. This may be due to the fact that the actual imperfection for each specimen was used in the theoretical predictions by the IC-method. A closer look at the results /33/ reveals that the uncertainty depends upon plate and stiffener slenderness:

- for stocky plates (normalized plate slenderness, $\beta = 0.9$)
 - the ECCS orthotropic approach seems over-conservative for the normalized stiffener slenderness, $\lambda < 0.8$
 - the ECCS column approach could over-estimate the strength for a very slender column ($\lambda < 0.2$)
- for slender plates ($\beta > 2.9$) all codes are conservative

When applying the model uncertainty in Table 3.1, it should be recognized that it somewhat accounts for variability of $e(x,y)$ and $\sigma_r(x,y)$. The uncertainty measures, hence, should be appropriately modified to reflect the real variability and the tolerance level set.

Table 1 Comparison of Model Uncertainty Based on 23 Tests of Axially Compressed Panels /31/

Code	Minimum Value	Maximum Value	Mean Value	COV (%)
BS5400 (1982)	0.89	1.46	1.10	13
DnV, Buckl. Notes 30.6 (1987)	0.94	1.52	1.10	16
ECCS (Column Appr.) (1990)	0.86	1.44	1.08	14
ECCS (Orth. Appr.) (1990)	0.94	1.68	1.14	15
Method proposed by Imp. College	0.94	1.34	1.10	08

The model uncertainty of the proposed IC method was also estimated by comparing predictions with this method with accurate numerical results for 63 panels. The resulting bias and COV of 1.05 and 5% are, as expected, less than 1.10 and 8%, previously obtained for the IC method. This is partly because imperfections etc. are more well defined in the "numerical test" panels. However, since the latter uncertainty measures do not contain any effect of parameter uncertainties, the bias and random uncertainty must be appropriately modified when applied to actual panels.

It seems that several prediction methods yield a reasonable accuracy for panels under axial compression. Moreover, the uncertainty varies with the slenderness of the plate and panel, and it could be further reduced by expressing it as a function of slenderness.

3.4 Stiffened panels subject to axial compression, bending or lateral pressure

3.4.1 Formulations

Some codes specify ultimate strength for panels under combined axial load (P) and bending, due to end moments or lateral load by ultimate strength interaction equations, such as Eq. (17). The DnV approach for combined axial lateral loading, q, in multispan stiffened plates is essentially such an approach using an equivalent moment equal to $qba^2/16$ (where a and b are plate length and width, respectively) and an assumed effective length of 60% of the span. This involves carrying out a stress check for each possible failure mode (that is PC, SC and ST; see Section 3.3.1) at the most critical section within the span under consideration. Considering both the normal and bending stresses in a simply supported strut under bending, the Perry equation (10), should be applied with /31,32/:

$$M = (M_{eq.} + P\Delta_o) / (1 - P/P_{cr}) \quad (11b)$$

$$M \cong M_q + (P(\Delta_o + \Delta_q)) / (1 - P/P_{cr}) \quad (11c)$$

for the case of end bending moments and uniform lateral pressure, q , respectively. M_{eq} is the equivalent bending moment for the case of variable moment. Δ_0 is the initial column deflection, and M_q and Δ_q are the bending moment and deflection at the midspan due to lateral load, respectively. When calculating the effective width for the plate element in cases with lateral pressure, the effect of lateral pressure b_e/b needs to be considered.

All the proposed equations (Eqs. 10-11) are related to a simply supported single-span model /31,32/, and they can be used to study axially compressed stiffened panels between column frames. However, a simply-supported single-span model is not appropriate for the design of multi-bay longitudinal stiffened panels subjected to axial and lateral loads, due to continuity effects and interaction in between adjacent spans having different initial imperfections.

The Perry model for the case with axial and lateral loads may be extended to clamped ends. While Eqs. (10,11a) are realistic for multispan panels when axial loads predominate, the clamped end case is expected to be a better approximation when lateral loads on multispan panels predominate.

The IC method /31-33/ deals with multi-span by introducing an additional deflection and an additional central span moment due to the lateral pressure acting on a fixed ended span. Then, each span (column) with its additional deflection and moment is calculated as an axially loaded simply-supported span.

Interaction equations such as Eq. (17), are more conservative than methods based on a stress check at critical sections (Eqs. 9-11), but are still more convenient for implementation in design rules since various forms and levels of bending can be catered for.

The Perry equations, however, are essentially a stress check at one point, and their use in complex load cases becomes involved. Reduced uncertainty usually may require a more complicated checking procedure. Hence, this refinement must be balanced against the consequences of potential errors made using the method.

Interaction curves of stiffened plates under combined plane compression and shearing stresses, was also investigated in /37/. Buckling, ultimate and fully plastic strength states are considered for flat plates and unidirectionally stiffened plates. Minimum stiffness ratio of stiffened plate for buckling (γ_{min}^B) and for ultimate strength (γ_{min}^U) are determined. For $\gamma < \gamma_{min}^B$, the buckling interaction curve is valid, for $\gamma_{min}^B < \gamma < \gamma_{min}^U$ the ultimate strength curve is valid, and, if the stiffened plate is stiff enough, a fully plastic strength interaction curve is proposed. Ultimate strength determination is based on stress coefficients that may be analytically evaluated using parametric formulae.

3.4.2 Uncertainty measures

There is very limited information about the uncertainties in the strength models for panels with axial and lateral loads. Comparisons have been made in /31/ between four experimental tests of the axial capacity for given lateral load levels and values predicted by the DnV and IC-methods. The ratio of test/predicted values ranged between 1.1 to 1.35 for the DnV approach and between 1.05 to 1.25 for the Perry formula (10, 11c). Interaction Eq. (17) yields even larger (conservative) bias factors.

3.5 Benchmark test of stiffened panels

Several classification societies and other organizations that have engaged in developing strength formulations for stiffened panels, were asked to determine the ultimate capacity of 10 multi-span stiffened panels which were selected by this ISSC committee. The focus was on the ultimate strength of (multi-span) stiffened panels located between transverse frames, failure modes and effective width of flange plating. Within the 10 panels, there are 8 longitudinally compressed panels and 2 subjected to longitudinal compression and lateral pressure. There are 6 Smith's panels /39/ (same geometries and actual imperfections) and 4 typical panels in the VLCC "Energy Concentration" ship that broke its back during discharge of oil in 1980 /40/.

The contributors to the benchmark study were first asked to analyze the 10 panels. Then all participants were informed about the outcome of all analyses and, if they wished, allowed to rerun their analysis /22/. The resulting model uncertainties are shown in Table 2. The names of contributors and codes/methods used, are made anonymous. The contributors are referred by one capital letter (A, B, C, etc.) and the codes by the symbols (M1, M2, etc.). The codes are in alphabetic order, BS5400 /9/, Bureau Veritas /10/, DnV /11,12/, ECCS column and orthotropic approaches /13/, Imperial College method /31/, Lloyds Register /41/ and Ueda-Yao's method /30/. Some contributors used codes as well as finite elements and other numerical methods. The latter types of results are not included in this summary.

It should be noted that the initial imperfections of the specimens have a large variation, and especially that the initial deflection of the stiffener for case 3 is two times larger than the tolerance. Initial plate deflections exceed the particularly restrictive tolerance requirement of the ECCS (column) code for all cases. Moreover, some methods had to be used outside their specified range of validity in this study. It was found that the effective width used in the various methods, differed by 0-15%, except for the method M6, which gave up to 45% lower value than other methods.

Some codes have been used by several contributors. It is

Table 2 Ultimate Strength to squash load for stiffened panels predicted by various organizations using different methods, obtained by the participants after being informed about the outcome of all first analyses.

Panel Reference No	CONTRIBUTORS										Mean	COV				
	METHODS/CODES	A	A	A	B	B	B	B	C	C			D	D	E	F
Boundary conditions		M1 No edge Stiff.	M2 No edge Stiff.	M2 With edge Stiff.	M1 No edge Stiff.	M2 No edge Stiff.	M3 No edge Stiff.	M4 No edge Stiff.	M5 No edge Stiff.	M5 Single beam column	M6 Single beam column	M6 With edge Stiff.	M7 No edge Stiff.	M8 Single beam column	M9 Single beam column	
	Pu/Po Experim. C.SMITH	Pu/Po	Pu/Po	Pu/Po	Pu/Po	Pu/Po	Pu/Po	Pu/Po	Pu/Po	Pu/Po	Pu/Po	Pu/Po	Pu/Po	Pu/Po	Pu/Po	
Smith 1.a	0.76	0.672	0.631	0.680	0.672	0.572	0.659	0.686	0.564	0.930	0.708	0.672	0.751	0.650	0.676	
Smith 2.b	0.83	0.800	0.812	0.832	0.803	0.764	0.811	0.797	0.833	0.930	0.812	0.803	0.543	0.870	0.800	
Smith 3.b	0.61	0.585	0.544	0.588	0.570	0.559	0.556	0.418	0.683	0.910	0.634	0.625	0.118	0.783	0.588	
Smith 4.a	0.82 (1)	0.703	0.689	0.703	0.693	0.652	0.664	0.560	0.784	0.940	0.775	0.771	0.508	0.870	0.719	
Smith 5	0.72	0.495	0.432	0.484	0.493	0.411	0.482	0.542	0.461	0.920	0.495	0.455	0.378	0.467	0.501	
Energ. Conc.	-	0.899	0.810	0.845	0.880	0.771	0.839	0.858	0.824	0.700	0.892	0.877	0.731	0.907	0.818	
Bottom Shell Energ. Conc.	-	0.798	0.794	0.819	0.791	0.735	0.752	0.804	0.802	0.850	0.870	0.858	0.874	0.689	0.798	
Upper Deck Energ. Conc.	-	0.928	0.843	0.863	0.923	0.813	0.887	0.892	0.893	0.880	0.924	0.915	0.923	0.881	0.888	
Side Shell																
Smith 1.b without lateral pressure with lateral pressure P=103.4kN/m ²	- 0.73	0.664 -	0.613 -	0.662 -	- -	- -	- -	- 0.512	- 0.529	- 0.930	0.684 -	0.645 -	- 0.670	- -	- -	0.662 0.636
0 Energ. Conc., Bottom Shell without lateral pressure with lateral pressure P=200kN/m ²	- -	0.889 0.871	0.810 -	0.845 -	0.880 -	0.771 -	0.839 -	0.858 0.660	0.824 0.774	0.770 0.700	0.892 -	0.877 -	0.731 0.820	0.907 -	0.818 0.707	0.106 0.119

(1) C. Smith panel 4.a has longitudinals interspersed with two tee-bars of 40 inches that are not considered by the contributors.

different contributors are different. Hence, this benchmark test shows two kinds of uncertainties: model (and parameter) uncertainties associated with the method for strength prediction, and uncertainties/"errors" associated with transforming the physical problem into the mathematical model handled by the method (i.e., modeling the geometry, boundary conditions, etc.), possible errors in the respective computer codes, use of the computer code, etc.

The benchmark study is described in more detail in /22/.

3.6 Stiffened girders subject to in-plane axial and bending stresses

3.6.1 General

Girders may be part of monocoque steel-plated structures as shown in Fig. 2. The flanges may be wide and stiffened; or narrow, unstiffened plates. The ultimate capacity of flanges with uniform in-plane loads is reviewed in Sections 3.2-3.3. However, it is noted that the stress in wide box girder flanges will be non-uniform due to shear-lag. Except for cases with very slender stiffeners, the effect of shear-lag on ultimate strength, however, can be ignored, as demonstrated, e.g., in the review /43/ and the recent study /36/.

The focus here is on the stiffened web subjected to in-plane axial bending or shear forces, and the interaction between the web and flanges. The international research effort in response to the box-girder bridge failures in the early 70's has led to the publication of numerous ultimate shear strength analytical models (based on the tension field approach), as well as some numerical models, which attempt to provide the most efficient and effective solution to the design of structures. Ultimate strength formulations for plate and box girders of civil engineering structures have recently been reviewed in /18,43,44/ and quantitatively assessed in /45,46/. As codes for marine structures have not been based on truly ultimate strength formulations, the review provided in Sections 3.6-3.7, is partly done as a tutorial presentation.

Currently, two approaches are applied in estimating the contribution to the ultimate capacity from the web subjected to in-plane direct and bending stresses:

- for webs with no stiffeners or transverse stiffeners connected to wide flanges (box girders) the contribution from the web is ignored (and the web capacity is utilized to carry shear forces); see, e.g., BS 5400 (Pratt truss approach)
- for webs with transverse or especially longitudinal stiffeners connected to narrow webs, the web is accounted for by a complete analysis of the load shedding from webs to flanges by means of an effective width approach.

Overall collapse is, by the current design practice, governed by failure of longitudinal load carrying stiffeners and flange failure. By assuming that the plate buckles between the stiffeners and flange, the effect of the plate can be accounted for by the effective width concept.

3.6.2 Plate failure modes

For unstiffened webs, the "efficiency" (η) of the compression zone, may be calculated by /18/:

$$\eta = (1 - 0.05(3 + \psi)/\lambda_p)/\lambda_p$$

This expression is a simple, generalized form of Eq. (9) for plates under uniform axial stress. The efficiency depends on the normalized web slenderness (λ_p) and the ratio (ψ) of axial stress in the upper and lower flange. Alternative expressions are also provided in /18/. The effective width method may also be employed for the case of longitudinally stiffened webs with the difference that each of the forming subpanels must be considered separately /18/. In addition, Cooper's formula /47/ is commonly used for doubly symmetric I sections (e.g., North America) as well as in the Cardiff approach (paragraph 3.7.1) /48,49/.

The information about the effect of perforations/cut-outs in girder webs on the capacity under direct stresses in bending, is limited, but the effect is also, especially for girders with longitudinal stiffeners, relatively small.

Local failure of narrow compression flange(s) and stiffeners are prevented by requiring that slenderness criteria are fulfilled. For instance, the width to thickness ratio of girder flange should satisfy the following criterion:

$$c/t_f \leq 18.5\beta\sqrt{235/\sigma_{of}}$$

where σ_{of} (in N/mm²) is the yield stress of the flange material. The semi-empirical Winter formula requires $\beta \cong 0.72$ and this value has been adopted in Eurocode 3 and in the Recommendations /18/. AISC /50/ specifies a value of $\beta = 0.75$ while BS5950 /51/ requires a value of $\beta = 0.76$. When the width to thickness ratio does not comply with the limiting value, the "effective" compression flange should be defined /44/. Similar local buckling criteria apply for stiffeners aligned in the direction of loading.

To avoid buckling of the flanges into the web, the depth, d to thickness, t_w should satisfy /18/:

$$d/t_w \leq 0.55\sqrt{A_w/A_f}(E/\sigma_{of})$$

where A_f is the cross-sectional area of the larger flange. (The web slenderness must anyway be restricted to reduce

of-plane "breathing" which can cause fatigue cracks under repeated loading conditions.)

3.6.3 Overall failure of narrow girder flanges and stiffeners

For girders with narrow flanges, the collapse of the flange out of the girder plane needs to be considered.

For plate girders with high web slenderness ratios, the pure torsion contribution is neglected and the critical torsional buckling stress is expressed only by the elastic warping resistance, $\sigma_{LT,cr}$. There is no general agreement on the formula to be used for the ultimate lateral torsional buckling stress. In Europe the following has been recommended /53/:

$$\sigma_{LT,u} = \sigma_o \left(1 + \lambda_{LT}^{2n}\right)^{-1/n} \quad (14)$$

with $n = 2.5$ and $\lambda_{LT} = \sqrt{\sigma_o / \sigma_{LT,cr}}$. Eurocode 3 indicates a value of $n = 1.5$ and suggests another approach based on a column buckling type curve. Formulae similar to the above are suggested in /19/.

Transverse stiffeners have a limited effect on the capacity under longitudinal direct stresses. Such stiffeners are more important in the case of predominantly shear loads and are, hence, discussed in Section 3.7.

Longitudinal stiffeners must be able to support the load shedding due to plate buckling in the web subpanels, up to the ultimate limit state, and must maintain nodal lines in a buckled web subject to shear. Hence, they must be appropriately sized. Experiments and numerical simulations indicate /44/ that the relative flexural rigidity ($\gamma_L = 10.92I_L/dt_w^3$) of the longitudinal stiffeners need to be increased beyond the optimum relative stiffness (γ_L^*), i.e., $\gamma_L \geq m_L \gamma_L^*$ where m_L is a semi-empirical amplification factor. The required rigidity depends, e.g., on the location of the longitudinal stiffeners, the aspect ratio of the longitudinally stiffened web panel, the web slenderness, the relative cross-sectional area of the stiffener and the web, the relative torsional rigidity of the stiffener (the effect of which is usually disregarded) and the type of loading /54/. In calculating the second moment of area about the neutral axis parallel to the web plate, an effective width of plate given by $b_e = t_w \sqrt{E/\sigma_{ow}}$ /18,44/ should be assumed.

Longitudinal stiffeners are load-carrying and a direct strength check may be more reasonable (BS 5400), e.g., considering a strut approach. However, in general, for girders subjected to both shear and bending, a stiffness or strength approach is recommended /44/.

3.6.4 Uncertainty measures

The uncertainty for direct and bending in-plane load expected to be as for the stiffened panels treated in Sect 3.2-3.3. The uncertainty associated with the BS 5400 approach for bending loading, was estimated to correspond to a bias COV of 0.988 and 4%, respectively /55/. Similarly, based on a sample of 18 test specimens, the bias and COV for the Com model was estimated to be 0.99 and 4-5%, respectively /56/.

3.7 Girders under predominantly shear stresses

3.7.1 General

Several theories to calculate the ultimate capacity of girders under shear, have been reviewed in detail in /44-45/. The general conclusion /46/ is that the Cardiff model /48/ represents the state-of-art. This view is also supported by the results of uncertainty analysis referred in Section 3.7.

The Cardiff model has been implemented, e.g., in the codes /9,14,51,52/, however, with slight modifications. BS5400 and BS5950 do not allow the use of tension field theory for longitudinally stiffened girders. EC3 does not cover longitudinally stiffened girders as yet.

The ultimate strength of girders in shear consists of the sum of three terms /48,49/ as shown in Fig. 4:

- (1) The elastic/inelastic critical buckling load V_1 of the webplate (beam action).
- (2) The load V_2 carried by the post-critical tension field (tension field action). The tension field contribution will be reduced by the presence of web perforations, especially if they are located at the geometrical center of the webplate.
- (3) The load V_3 carried by the flanges at the instant of plastic hinge formation in the flanges (Vierendeel mechanism).

From vertical equilibrium, the ultimate strength in shear of a plate girder is determined by (Fig. 4):

$$V_{ult} = V_1 + V_2 + V_3 = V_{cr} + 0.5\sigma_t^o t_w \sin 2\theta(d - b \tan \theta) + \sigma_t^o t_w (c_c + c_t)$$

where σ_t^o is the tension field stress to cause yielding of the web material in the tension band (based on the von Mises yield equation); d and t_w are the depth and thickness of the web; b is the distance between transverse stiffeners; θ is the inclination of the tension band to the horizontal; and (c_c, c_t) are the anchorage lengths of the tension band on the compression and tension flanges, respectively.

and tension flanges, respectively. c_c and c_t identify the positions of the plastic hinges. The latter are dependent on the flange rigidities which are themselves influenced by the presence of any direct and bending in-plane stresses.

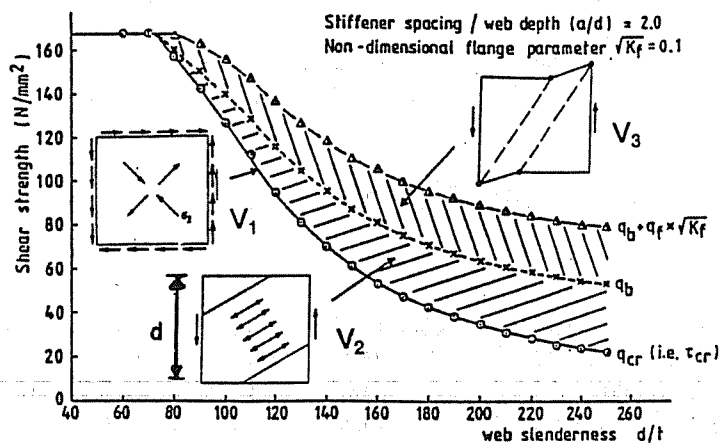


Fig. 4 Contributions to the ultimate shear strength of a plate girder /48/.

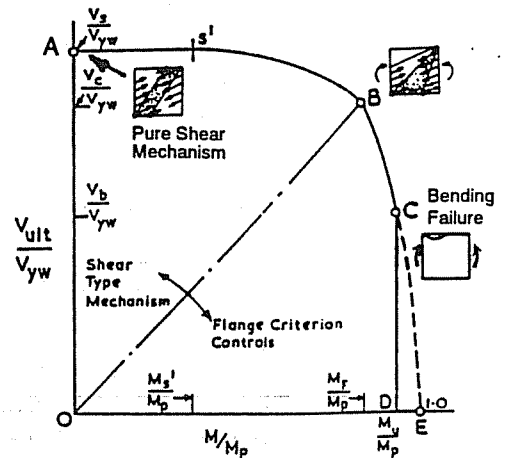


Fig. 5 Interaction curve between shear and bending effects /45/.

The Cardiff model has been validated for plate girders with narrow, fairly thick flanges (see Section 3.7.5). The third term (V_3) may not be fully developed in box girders with wide, thin flanges, by using the "conventional" effective width of the flanges. Hence, limited use of the plastic frame mechanism action is recommended for box girders in, e.g., BS5400; see /43/. If V_3 is neglected, the Cardiff model effectively reduces to the Basler model /44,48/.

Transverse stiffeners affect all terms in the expression, and are crucial to the shear capacity. Longitudinal stiffeners are only accounted for by their influence on the critical buckling stress of the web, and hence the term V_1 . Although the Cardiff model does not represent the most accurate approach /18/, it is recommended in /18,57/ because of its simplicity.

3.7.2 Effect of direct and bending in-plane stresses - interaction between shear and bending

Any direct and bending in-plane stresses affect the membrane stress tension field σ_t^o and the plastic moment capacity M_{pf} of the flanges, in addition to the critical buckling stress of the web plate.

The stress resultant of the diagonal tension band gives rise to a horizontal component in the flanges. The Cardiff model does not account for the effect of this horizontal component on the bending capacity of the flanges, while /46,58/ propose to do so. However, the Cardiff model makes allowance of axial stresses in the flanges caused by in-plane girder bending and axial forces.

Interaction between shear and bending and direct axial stresses is accounted for by the Cardiff model using a diagram as shown in Fig. 5. Parts AC and CD are based on the shear capacity (Section 3.7.1) and bending (direct stress) capacity (Section 3.6), respectively. A transition in failure mode occurs at point B, where the applied bending moment is assumed to be solely carried by the flanges. Between points S' (where $M_s \sim 0.5 M_p$) and B; and B and C, the curve may be represented by parabolas, or, without much loss of accuracy, straight lines. Points D and E refer approximately to first yield and plastic moment, respectively.

3.7.3 Stiffener requirements

The shear capacity can be achieved only if the stiffeners fulfill certain stiffness and strength requirements.

Transverse stiffeners (including an effective width of web) should fulfill stiffness requirements analogous to those mentioned for longitudinal stiffeners in Section 3.6. However, transverse stiffeners carry compression forces equal to the difference in predicted ultimate strength (V_u) of the girder and the critical buckling strength of the web panel in shear acting in the plane of the web. The eccentricity to the stiffener's neutral axis of the loads introduces an additional bending moment in the stiffener. In addition, the out-of-straightness of possible longitudinal stiffeners (in the compression zone only) causes a destabilizing moment in the transverse stiffener. The intensity of each transverse force is recommended to be taken as 1% of the compression load in the longitudinal stiffener (without any web effective width) /44/. The strength of the transverse stiffeners is then verified by the beam-column approach, similar to those outlined in Section 3.3, using a buckling length of 70% of the stiffener depth /18,44/. Some transverse stiffeners may have to carry point loads from other major components, e.g., in frame corners. An additional stiffener requirement for transverse stiffeners is briefly reviewed in /44/.

Longitudinal stiffeners should fulfill certain stiffness and strength criteria, considering the destabilizing effect of shear stress.

3.7.4 Effect of web cut-outs

Significant information only exists for shear loading with very low axial bending stresses and for vertically stiffened plate girders containing one cut-out per panel. Accurate formulations for special cases with (reinforced) cut-outs are presented, e.g., in /59,60/.

The ultimate capacity can be assessed approximately by linear interpolation between the unperforated ultimate strength (V_u) and the Vierendeel (frame mechanism) load (V_v) /60/. Hence:

$$V_{ult} = V_v + (V_u - V_v)(1 - D/d) \quad (16)$$

where D/d is the ratio of the opening diameter to girder depth. As mentioned before, this approach has been validated for plate girders where the relatively heavy flanges provide bending capacity in the frame action.

3.7.5 Uncertainty measures

Uncertainty measures for plate girders under shear loading are given in Table 3.

Table 3 Model uncertainty for stiffened girders (without cut-outs) subject to shear loading

	Cardiff	EC 3 ²	BS 5400 ¹	EC 3 ²
Ref. Sample	/46/ 164/67	/46/ 164/67	/62-63/ 102	/62-63/ 109
Bias	0.98/1.00	1.08/1.09 ³	1.14/1.6	1.10
COV (%)	6/7	16/13 ³	16/36	14.5

¹⁾ BS 5400 for longitudinally stiffened panels is not based on ultimate limit state and tension field approach.

²⁾ EC 3 do not provide criteria for longitudinally stiffened girders.

³⁾ Refers to evaluation of model developed in Germany for longitudinally stiffened girders, for inclusion in EC 3.

While the uncertainties for the girder models presented in Table 3 are determined for "all available" data, a closer examination of the results shows that the uncertainty depends, for instance, upon the web slenderness b_w/t_w . The COV for b_w/t_w less than 250 is about twice that for larger slendernesses (up to 400) /46/. By comparing the model uncertainties with and without accounting for the effect of the horizontal component of the tension field force in the flanges, the effect of these different formulations is found to be negligible. Also, it is observed that the slightly different versions of the Cardiff model implemented for transversely stiffened girders in EC3 and British standards do not yield very different model uncertainties.

The BS 5400 model for longitudinally stiffened girders is based on empirical considerations /63'/ conducted before the accuracy of the Cardiff model for such girders had been proven.

The simplified approach, Eq. (16) mentioned above for accounting for cut-outs implies a bias and COV equal to 1.60 and 0.35, respectively. The more refined formulations for circular and rectangular cut-outs with/without reinforcement typically yield bias' in the range 0.83 to 1.07, and COV's between 6 and 17% /56,59-61/.

4. ULTIMATE STRENGTH OF CYLINDRICAL SHELLS

4.1 Introduction

Cylinders are frequently used in offshore platform structures. Significant research on the ultimate strength of cylindrical columns and beam-columns was accomplished for civil engineering structures in the 1960-70's, see, e.g., /20/, and for local failure modes of more thin-walled cylinders in aerospace structures in the 1960's; see, e.g., /64/. However, the more "stocky" geometry and the radial pressure loads acting on offshore structures were not considered until the late 1970's and 1980's, partial reliance being placed on long-term research relating to submarine shells /65/.

Cylinders in offshore platforms may suffer both local and overall failure. The relatively long, unstiffened thick-walled tubulars used in bottom supported platforms exhibit overall failure; however, for deep water platforms, external pressure affects the strength. Thin-walled, stiffened tubulars used in floating platforms primarily suffer local failure modes, which are particularly sensitive to imperfections.

4.2 Overall column and beam-column collapse

4.2.1 Failure modes and formulations

With the relatively stocky cross-section of members used in bottom supported platforms, overall collapse is of primary concern. For the design for local buckling, cross-sections are normally classified into four groups as follows:

- plastic full plastic action can develop and maintained through significant rotations
- compact plastic hinge capacity can be achieved but limited rotations only
- semi-compact yield can develop at the extreme fibers
- slender local buckling occurs limiting flexural capacity.

The slenderness limits applicable to each group can vary depending on the structural action although this subtlety is frequently ignored.

4.2.2 Column capacity

The capacity of compression members is determined by the interaction between buckling and yielding, and depends primarily upon yield strength, geometrical imperfections, as well as residual stresses (and, hence, the fabrication method) as represented by column curves in Fig. 7 /74/. The effect of residual stresses vanishes at high slenderness, λ , since

total (including residual) stress is less than the proportional limit. For really high slendernesses, both effects vanish and the capacity approaches the ideal elastic buckling strength.

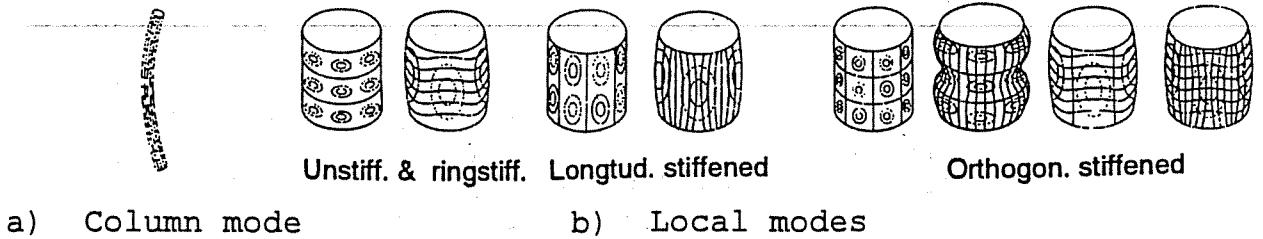


Fig. 6. Buckling forms of cylindrical shells, see e.g. /11/.

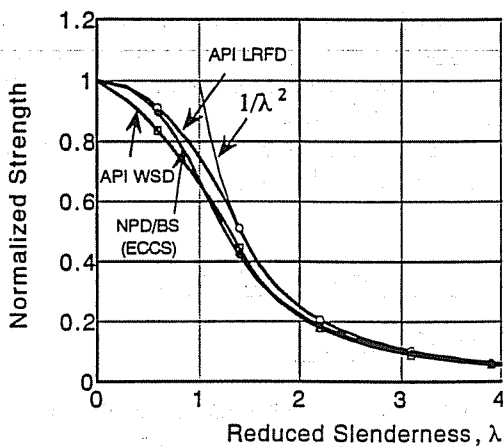


Fig. 7 Column curves

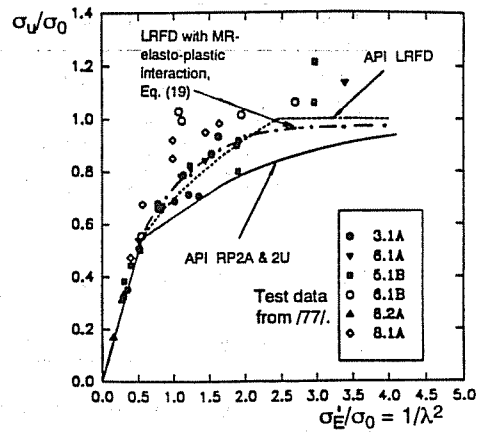


Fig. 8 Local buckling capacity under hoop compression.

Typically, differences in cross-section shape and plate thickness will influence the residual stress (and the ratio of I and A), and multiple column curves are applied. For tubular beam columns in offshore structures, there is no distinction between hot- and cold-formed tubulars /75/. Some codes (e.g., API LRFD, and some class society rules) are based on the SSRC Curve 1, while others (BS5950, DnV, NPD) apply the ECCS curve. The SSRC curve is similar to a Johnson-Ostenfeld correction to the elastic buckling stress. This curve follows the Euler curve for $\lambda > \sqrt{2}$. It may be interpreted as a correction for residual stresses (tangent stiffness formulation). The ECCS curve more explicitly accounts for both residual stresses and geometrical imperfection. In principle, a reduced yield stress should be used when applying the European column curve to fabricated columns. However, since offshore tubulars are constructed by cold rolling (which enhances the strength in the first place) and welding, this reduction is dispensed with. It is noted that API WSD is based on the AISC WSD, and is considered to be somewhat conservative for tubulars in offshore structures. This is because it is based on WF-shapes that possess high residual stresses compared with, e.g., cold-formed tubulars.

4.2.3 Bending

If D/t satisfies the requirement to fully plastic cross sections, the plastic moment is applicable (API codes, BS5950). For larger D/t the appropriate reduction due to local buckling is applied; see Section 4.3. NPD/DnV refer to the first yield stress for the whole D/t range.

4.2.4 Axial compression and bending

Interaction between axial compression (σ_a) and bending (σ_b) is established in some codes (API, DnV tubular member design) by:

$$\frac{\sigma_a}{\sigma_{au}} + \frac{C_M \cdot \sigma_b}{\sigma_{bu} \left(1 - \frac{\sigma_a}{\sigma_E}\right)} = 1.0$$

where σ_{au} is determined by the appropriate column curve, σ_{bu} is the ultimate stress under pure bending and σ_E is the Euler buckling stress. C_M is a factor to account for the variation of (first order) bending stress along the member.

In addition to the overall "stability" limit state, (17) there are local yielding and buckling criteria. For columns experiencing plastic strains before collapse, interaction between local and global behavior is complex.

The ECCS interaction equation is based on a Perry-Robertson approach. The axial capacity, σ_{au} is represented by two terms $\sigma_a + e^* \sigma_a / (1 - \sigma_a / \sigma_E) = \sigma_{au}$, such that it corresponds to the column curve by suitably choosing a fictitious eccentricity e^* to account for the reduction in strength due to imperfections and residual stresses. The interaction equation for axial compression and bending is then [ECCS; e.g., NPD/DnV]:

$$\frac{\sigma_a}{\sigma_0} + \frac{e^* \sigma_a + C_M \sigma_b}{(1 - \sigma_a / \sigma_E) \sigma_0} = 1.0$$

If the plastic bending capacity is utilized in bending, (18) should be modified by increasing e^* and σ_0 in the second term by the ratio of the plastic to elastic section modulus. Often a conservative value of C_M is used in many codes, especially when the first order moments cause the beam-column to bend in an S-shape.

4.2.5 Axial compression, bending and hoop stress

Current codes do not account for the combined effects of external pressure, axial compression and bending loads on columns, or they represent this interaction poorly, e.g., API 2U. Such effects are important for deep-water platform

Loh /76/ modified the (elasto-plastic part of the) RP2A column curve and the moment capacity to account for external pressure.

4.2.6 Uncertainty measures

Uncertainty in overall column curves is given in Table 4.

Table 4 Uncertainty in the ultimate capacity of columns under compression

Formulation	Data	No. of specimens	Bias	COV (%)
API RP2A	/77/	56	1.14	7
API LRFD	/77/	56	1.02	8
ECCS (DnV/NPD)	/74/	280	see 1)	5-16 ¹⁾

¹⁾The bias may be represented by $B = 1.0 + 0.1 \lambda$ (for $\lambda \leq 2$) and $B = 1.0$ (for $2 < \lambda < 3$) and the COV also varies depending upon the reduced slenderness, λ .

It is seen that the LRFD approach corresponds better to the mean of experimental results than the RP2A (WSD) approach. The random uncertainty (COV) for the relevant formulations is seen to be relatively small.

Ref. /78/ provides an estimate of the model uncertainty for tubular beam-columns which have so small cross-section slenderness that local buckling effects have an effect. By using Eq. (17) with σ_{au} and σ_{bu} that account for local buckling, the linear interaction between axial and bending stresses that include second order effects, is found to have a bias of the order 1.1.

The Loh correction of the LRFD-column curve for hoop compression yields a bias of 1.07 and a COV of 6%, while the corresponding formulation for bending capacity implies a bias and COV of 1.24 and 7%, respectively. The latter uncertainty is reflected in a bias of 1.23 and a COV of 14% for beam-columns subjected to axial compression and bending under hoop compression.

Code formulations for ultimate bending capacity and axial-bending under hydrostatic pressure, should be improved.

A crucial factor in applying the column curves is the effect of boundary conditions, as taken into account by the K-factor. Often this is done for offshore structures by using a constant value for braces and legs of jackets. This implies a significant conservative bias and some variability /79/.

4.3 Local buckling of unstiffened and ring stiffened shells

4.3.1 Failure modes

Frequently, codes for ring stiffened shells specify stiffness requirements for the stiffeners to prevent stiffener collapse until the shell has failed. Hence, interframe failure is generally of concern. Nevertheless, explicit ultimate strength criteria are given for densely stiffened cylinders; see Section 4.4. Generally, the API codes LRFD, WSD and 2U differ although it should be observed that the former two codes are applicable for $D/t < 300$ while Bul. 2U is also valid for more slender shells.

4.3.2 Axial compression or bending

Axial compression stresses cannot reach yield if $D/t > 30$ for $\sigma_a = 240$ MPa, and the bending capacity will be less than the plastic moment if $D/t > 30-50$ for $\sigma_0 = 360-240$ MPa, while the capacity under external pressure is essentially a local failure mode.

The three API formulations /WSD, LRFD, 2U/ provided for local buckling under axial load is based on the classical elastic buckling formula in the elastic range. In the inelastic range the strength is expressed as a function of D/t , which is fitted as a lower bound to experimental data. The NPD/DnV code uses a Merchant-Rankine approach /80/ to represent the interaction between elastic buckling and yielding. Cho and Frieze /81/ propose to improve the correlation with test results by using a knock-down factor, ρ on the elastic buckling strength:

$$1/\sigma_u^2 = 1/\sigma_0^2 + 1/(\rho\sigma'_E)^2 = 1/\sigma_u^2 = 1/\sigma_0^2 + 1/(\rho\sigma_E)^2 = (1 + \lambda^4)/\sigma_0^2$$

where σ_u , σ_0 and σ_E are the ultimate, yield and elastic buckling strengths, respectively. λ is the normalized slenderness given by $\lambda^2 = \sigma_0/\sigma'_E$.

4.3.3 Hoop compression

The hoop capacity is described by the elastic buckling formulae for $D/t > 60$ for mild steel; the API-WSD and 2U formulations are a lower bound and LRFD a mean fit to test results in the elasto-plastic regime, described by several expressions. The NPD approach is again based on the MR approach and is below the API predictions, because the σ_E used is conservative. A modified MR method can be used to replace the capacity by a single expression over the whole D/t range /81/. Fig. 8 shows σ_u/σ_0 vs. $1/\lambda^2$ using σ'_E and σ_u given by API and Eq. (8) respectively. For D/t between 10 and 40 (a relevant range for pipelines and tethers), a Timoshenko formulation, which is essentially a stress check of an imperfect ring, is found

yield a good estimate, e.g., better than consideration of a plastic mechanism /82/.

4.3.4 Axial loading and hoop compression

API codes specify different interaction equations for all combinations of axial tension/compression and bending and hoop compression. For instance, the interaction between axial and hoop compression is described by a quadratic relationship in 2U, while WSD and LRFD take the smallest values implied by the interaction equation for elastic buckling and the elasto-plastic buckling capacities for individual loads.

NPD/DnV is based on a generalization of the Merchant-Rankine formula for interaction between elastic buckling and plastic yielding /80/. The advantage of this approach is that it allows also tensile loads to be easily handled and that it converges into linear interaction and the Von Mises-Hencky interaction for large and small D/t, respectively.

A further development of this method for combined axial and hoop compression was made in /81/ by calibrating knock-down factors on the elastic buckling stresses against test data.

For shells under axial compression and radial pressure, the effects of the various parameters controlling strength such as L/R, R/t, L/t, and E/σ₀ were examined with a view to identifying those important for inclusion in knockdown factors. The effects were found to differ markedly between the two actions, but bearing in mind a preference to use the same parameters within all of the knockdown factors in order not to complicate the equations, the parameter chosen was (E/σ₀)√Z, where the Batdorf slenderness parameter Z = (L²/Rt)√(1 - ν²); R = D/2 is the mean shell radius.

The determined equations in the presence of axial stress σ_x and hoop stress σ_θ were:

$$\left(\frac{\sigma'_x}{\rho_x \sigma_{xc}} + \frac{\sigma'_\theta}{\rho_\theta \sigma_{\theta c}} \right)^2 + \left(\frac{\sqrt{(\sigma_x^2 - \sigma_x \sigma_\theta + \sigma_\theta^2)}}{\sigma_0} \right)^2 = 1.0 \quad (20)$$

where σ'_x = σ_x for σ_x < 0 and = 0 for σ_x ≥ 0, σ'_θ = σ_θ for σ_θ < 0 and = 0 for σ_θ ≥ 0.

Clearly, this approach can be extended to other combinations of loads, but different knock-down factors will then have to be applied for a given load in different combinations to achieve a best fit.

4.3.5 Uncertainty measures

The model uncertainty for current API codes (especially the LRFD approach) have been estimated by data reported in

/77/. Experimental results for ring stiffened cylinders compiled in /81/ and used to assess the uncertainty of modified Merchant-Rankine formulation, BS5500 and an version of the DnV formulation, where appropriate. While nominal geometrical data and yield stress are given for specimens, no information is given about initial imperfect and residual stresses.

Because a number of tests on single bay and stiffened shells also had been conducted, the effects of these particular factors were also examined in detail.

Among the API codes, 2U was found /79/ to give the best fit to data for local buckling under axial compression, with a bias and COV of 1.07 and 8%, respectively. The NPD/DnV approach for this loading yields a bias and COV of 1.59 and 32%, respectively. However, as shown, e.g., in /81/, the uncertainty increases with slenderness, suggesting that applying correction factors on the elastic buckling stress would improve the accuracy. By using such a modified approach a bias and COV of 1.05 and 14% was achieved /81/. For different data bases applied in estimating these uncertainties should be observed.

For bending the API LRFD formulation, which converges to the nominal plastic capacity for small D/t , yields a best fit to data within $15 < D/t < 80$, with a bias and COV of 1.16 and 9%, respectively. Hence, there is a significant reserve capacity beyond the plastic moment of an ideal plastic material, essentially due to strain hardening. However, another investigation /82/ for long cylinders with $10 < D/t < 40$ shows that the bias and COV are 0.87 and 7%, respectively. For this D/t range, it is demonstrated that other approaches, e.g., used for pipelines by Shell, yield a better fit.

The local hoop buckling stress in the elastic region is approximately the same for the API WSD, LRFD and 2U. The LRFD equation gives significantly higher stresses in the inelastic region than the "lower bound" estimates that WSD and 2U provide. The bias and COV of the LRFD is 1.12 and 16%, respectively, by using data for D/t in the range 30 to 80. The NPD/DnV approach is found to yield a bias of 1.15 and a COV of 8%. The corresponding numbers for the ECCS approach are 1.21 and 11%. For more thick-walled tubulars ($10 \leq D/t \leq 40$) the Timoshenko formula is found to yield a good fit /82/.

Comparison of the three API formulations for axial tension-hoop compression shows that the LRFD formulation yields the smallest bias with 1.2, while the COV of 16% is slightly larger than that for the 2U method, which has a bias and COV of 1.3 and 14%. A closer look at the results shows that the LRFD predicts the inelastic capacity well, while the discrepancy for long ("unstiffened") shells show a bias of the order 1.4. While the initial NPD/DnV-CNB formulation yields a bias and COV of 1.50 and 13%, a modified MR-formulation yields a bias and COV of 1.16 and 9%, respectively.

The uncertainties in the three API formulations for interaction between axial and hoop compression are quite close; with, e.g., a bias and COV of 1.15 and 10% for API LRFD. The bias of 1.45 and COV of 20% in the NPD/DnV-CNB approach can be reduced to 1.03 and 8%, respectively, by introducing knockdown factors on the elastic buckling formulae.

For interaction between bending and hoop compression the API formulations, LRFD and 2U represent the extemities, with a bias and COV of 1.29 and 14%; and 1.44 and 8%, respectively.

An examination of stress relieved ring stiffened shell data demonstrated that, while residual stresses had little effect on axial compressive strength, under increasing levels of radial pressure, the shells exhibited increasing strength, up to 37%, in the case of pure radial pressure. It was assumed that stress relieving allowed substantial moments to develop at the frames in contrast to when residual stresses were present and yielding over the frames began early in the loading history thereby inhibiting the development of significant boundary moments.

4.4 Frames in ring stiffened cylinders

Among the API formulations, the 2U approach seems to be a refinement of the other formulations. This is also borne out by the model uncertainties determined /77/. The model uncertainty of 2U is clearly smaller, amounting to a bias and COV of 0.96 and 6.8%. Since this sample is small, a statistical uncertainty should be added. Since the LRFD and WSD approaches are based on buckling in two modes in the circumferential direction, they become very conservative for high buckling modes. The BS 5500 approach is also considered relevant for shells subjected to radial or hydrostatic pressure, while for axial loading the NPD/DnV-CNB may be suitable. However, no uncertainty measures are available.

4.5 Orthogonally stiffened shells

4.5.1 Failure modes and formulations

A wide range of failure modes can occur in orthogonally stiffened shells, involving the shell and stiffening elements in isolation and in combination. Thus the shell alone can buckle, the shell and longitudinal stringers combined can suffer interframe buckling, the stringers and frames alone can trip, and the shell, frames and stringers can suffer general instability - orthotropic buckling. The stiffened shell may itself not buckle, but it can suffer overall column buckling. As for ring stiffened shells, the frames are generally designed not to fail. Stringers can be proportioned not to fail in a local or overall lateral torsional mode.

The most relevant formulations for orthogonally stiffened shells in marine structures are API Bul 2II /68/, DnV-CNB /11/

ECCS /73/ and RCC /83/. Approaches based on discrete stiffeners and orthogonal shell theory are given.

This review is to a large extent based on a comprehensive study /84,85/.

4.5.2 Axial loading

API Bul. 2U calculates the strength of the shell plating under axial compression based on the theoretical elastic buckling stress, a knock-down factor which (implicitly) accounts for imperfections and inelastic behavior due to collapse. The axial capacity of the stiffened panel is determined by first calculating the elastic buckling stress for the plate and stiffener separately. The elastic buckling stress of the stringer is determined by assuming it to be simply supported, including an effective width of the shell with a reduction factor for residual welding stresses. The elastic buckling of the stiffened panel is then calculated as the sum of the two contributions, and the collapse strength is obtained by using the Ostenfeld-Bleich tangent modulus approach. The resulting stress σ_{ic} is used to calculate a revised slenderness parameter and an effective width, b_{em} . The ultimate axial capacity, σ_u is then

$$\sigma_u = \sigma_{ic}(A_s + b_{em} t) / (A_s + bt)$$

when the ultimate force is averaged over the total cross-section area.

The RCC approach, which preceded Bul. 2U, follows the same procedure, however, with a modified elastic buckling stress and knock-down factor for the plating, and introducing reduction factors for residual stresses depending on the weldment.

The ECCS approach is similar to that of the above mentioned codes, but uses a less refined knock-down factor for shell buckling. The DnV approach (formulation C) deviates from the API/RCC methods by referring only to the stiffener with an effective shell, rather than to contributions from both stiffener and shell, and like to ECCS approach, by using similar "knock-down" factors.

4.5.3 Radial loading

The formulation for radial loading is analogous to that for axial loading.

API Bul. 2U predicts the ultimate capacity by superposing the buckling pressure for the (unstiffened) shell and the plastic collapse of the ring stiffener including an effective flange width, with a knock down factor.

The RCC approach is based on the plastic capacity of the ring stiffener, using several empirical geometrical correction

factors, and an Ostenfeld-Bleich tangent modulus to account for plasticity. However, the effective flange of the shell considered seems to be small.

The NPD/DnV-CNB and ECCS approaches for radial pressure are similar to those used for axial load, however, using the appropriate theoretical buckling coefficients.

4.5.4 Combined axial and radial loading

API Bul. 2U recommends the following ultimate strength interaction equation for combined axial load and radial load

$$R_x^2 + CR_x R_0 + R_0^2 = 1 \quad (22)$$

where R_i is the utilization ratio for load no. i). The initial RCC approach used a different quadratic interaction function. However, in the recent study /84/, Eq. (22) was recommended, but with a different C than in the RCC formulation.

DnV-CNB uses a generalized Rankine-Merchant approach described above for unstiffened shells.

4.5.5 Uncertainty measures

Table 5 shows the model uncertainties estimated in /84/ using a selection of available test results for orthogonally stiffened cylinders. It is shown particularly that aluminium shells tested for aerospace structures failing by elastic buckling are not relevant for validating prediction methods for offshore structures. Also, a closer look at the model uncertainties, reveals that they vary depending upon which test sample is considered. For instance, the bias of the RCC formulation for axial load is 1.13 using 6 small scale specimens (IC1-6) and 0.93 when using 5 specimens B1-5. This fact may be related to differences in residual stresses and geometrical imperfections, even if imperfections were reported to be within the tolerance level.

Among the methods compared, the RCC method gave the best fit. Various possible improvements of the RCC formulation for axial capacity were investigated in /84/, but only resulted in minor reductions in the model uncertainty. The NPD/DnV-CNB formulation is not satisfactory for radial and combined loading. The large bias and COV are attributed to considering the shell unstiffened when the Batdorf width parameter $Z_s < 8.586$. If the more applicable narrow panel DnV model for axial compression is used, the figures would probably improve. Even if the RCC model for radial load implies a small uncertainty, it is observed in /84/ that this is partly due to using adjustment factors to fit the limited test data available. Hence, further improvement of the basic formulation is necessary. It is also desirable to improve the interaction equation to reduce the random uncertainty (COV).

Table 5 Model uncertainties estimated by comparison with results for steel shells /84/

Load: Test data ¹⁾ : Code	Axial load		Radial load		Interaction	
	48 specimens		11 specimens		38 specimens	
	Bias	COV (%)	Bias	COV (%)	Bias	COV (%)
API 2U						
- discrete	1.02	14	1.21	15	1.13	16
- orthotropic	0.86	25	0.87	46	-	-
RCC	1.02	14	0.97	10	1.09	25
DnV-CNB ²⁾ (1984)	0.97	21	1.40	39	1.68	25
ECCS (1983)	1.21	24	-	-	-	-

¹⁾ σ_0 : 310 to 510 MPa; R/t: 95 to 505; L/R: 0.64 to 4.8; s/t: 25 to 130.

²⁾ Only DnV-CNB formulation C (orthotropic theory) is applied.

It is noted that the bias of the API Bul. 2U and formulations for axial or radial loads is practically invariant with respect to the predicted strength to squash load, the for the other formulations decreases towards 1.0 increasing strength (slenderness).

The advantage of the general interaction approach used in DnV-CNB is that it converges to the von Mises-Hencky yield criterion and linear interaction for stocky and slender structures, respectively. A further advantage is that it accounts for the effect of tensile stresses. However, the fact that the bias/COV varies with the slenderness suggests that the formulation may be improved by introducing additional knockdown factor on the elastic buckling stress, demonstrated for unstiffened/ringstiffened shells in Section 4.3. However, it is desirable to do this based on better information about imperfections and residual stresses, also in view of the magnitude of such fabrication factors in actual structures.

Finally, it is noted that formulations for tripping failure of stiffeners in general is based upon a hinge between stiffener and shell plating. DnV-CNB allows using an elastic restraint on the stiffener, but the fact that shell buckling may initiate stiffener failure, is not yet covered.

5. ULTIMATE STRENGTH OF TUBULAR JOINTS

5.1 General

Joints between panels, and rectangular tubulars with the same width can be designed (with diaphragms) to transfer forces by membrane actions, and the ultimate strength may be fairly easily estimated. Joints between cylindrical members have a much more complex - shell - behavior. Such joints may be classified as follows:

- unstiffened, plane joints
- unstiffened, multiplane joints
- stiffened joints
- grouted joints

Current codes /16,17,66,67,86-88/ specify parametric formula for unstiffened, plane K, T, Y, X shaped joints, corroborated by tests. Other joints, e.g., plane KT and DT and multiplane joints, need to be considered on a case basis. Other unstiffened joints are usually classified based on the geometry and loading, see, e.g., Fig. 9b. General reviews of ultimate strength of tubular joints may be found in, e.g., /86,90/.

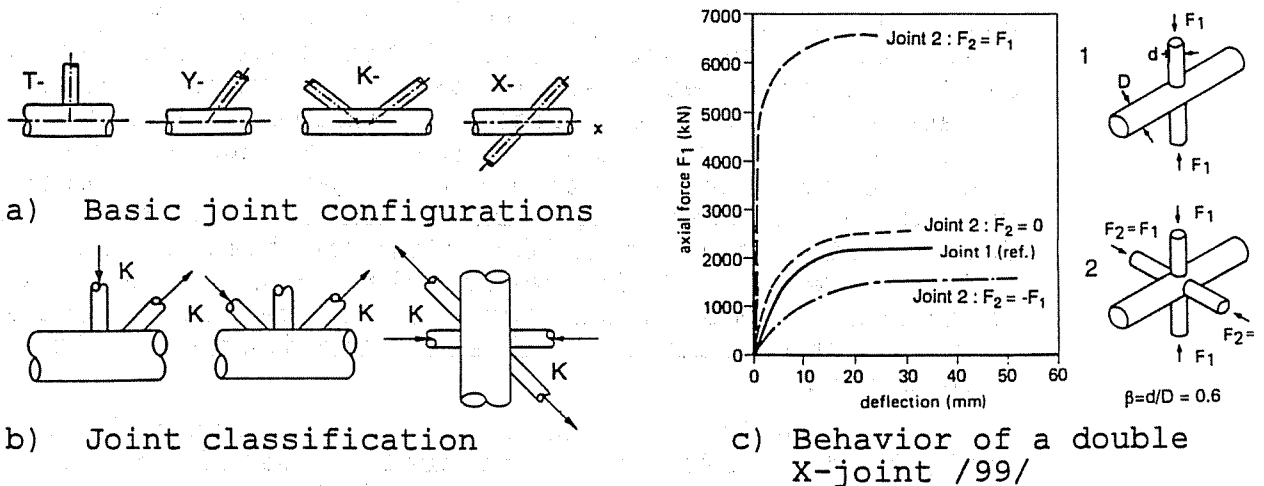


Fig. 9 Tubular joints

Depending upon material and geometrical properties, ultimate failure of a joint may occur due to buckling (due to compressive loading), excessive deformation, fracture or gross separation, shear failure of the chord-brace joint, lamellar tearing (of thick chords). For Y- and T-joints, it is, therefore, distinguished between compression and tensile loading. Different definitions of crack size that implies tensile failure have been used. While API, CSA, NPD and DnV use first crack, HSE /16,91/ refers to ultimate load capacity. The former approach is conservative for static loading, but is convenient to avoid consideration of interaction between fatigue and fracture. In case of tension and interaction between tension and in- or out-of-plane bending, the joint does not exhibit a distinct limit capacity in the load-deflection

behavior and the limit state should be given by maximum deformation, and possibly maximum strain (to avoid fracture

By merging all failure modes in one ultimate limit state it is important to ensure ductility, especially for materials with yield stress, σ_0 , exceeding 400 Mpa. Different codes specify the ratio σ_0/σ_u in the range 0.70 to 0.83.

Current formulations have been established by fitting parametric formulae to experimental data. Recently, systematic studies using nonlinear finite element methods have also been used to generate a data basis for fitting ultimate limit state equations. While API adopts a pragmatically determined lower bound of test data, European codes are based more on statistical analysis to determine mean and 5% fractile curves.

5.2 Formulations for simple joints

Strength provisions in the API WSD/LRFD codes are widely used. They contain parametric formulae established on the basis of a lower bound on experimental data selected in /92/. The formulae are generally of the form /66/:

$$P_u = Q_u Q_f \frac{\sigma_0 T^2}{\sin \theta} \quad (2)$$

$$M_u = Q_u Q_f \frac{\sigma_0 T^2}{\sin \theta} (0.8d) \quad (3)$$

in which σ_0 and T are the chord yield stress and thickness; Q_u and Q_f are nondimensional factors for brace load and chord stress effects, respectively. These factors are functions of the ratios of the diameters of the tubulars, of diameter to plate thickness etc.

The following interaction equation is recommended by API

$$1 - \cos \left[\frac{\pi P}{2 P_u} \right] + \sqrt{\left(\frac{M}{M_u} \right)_{IPB}^2 + \left(\frac{M}{M_u} \right)_{OPB}^2} = 1.0$$

where IPB and OPB refer to in- and out-of-plane bending.

Since the review /92/ was accomplished, new data have become available and data used before, have been rendered obsolete. New data bases have been established by /93/ and /94/. Other code formulations have been proposed by, e.g., HSE, DnV, and NPD. In particular, improved formulations have been introduced for X-joints and in-plane bending. Also, Canadian and European codes refer to a 5% (or 95%) fractile instead of a lower bound.

The deviation of the NPD formulation from, e.g., API is partly caused by NPD introducing the constraint that the design values shall be obtained from the characteristic values using the same material (safety) factors.

Instead of Eq. (24) other codes apply an interaction which is linear in the axial force and out-of-plane moment and quadratic in terms of the in-plane moment.

It is also noted that the strength formulae given in various codes have different range of validity.

In view of the harmonization of offshore codes, a new data basis /95/ was established by a critical screening of existing data, and recommendations on selection of formula were given in /96/. See also Table 6.

In particular, API LRFD /66/ applies a Q_u (in Eq. (23)) for in-plane bending, which is $Q_u = 3.4 + 19\beta$, where β is the ratio of brace and chord diameters. Other codes (e.g., DnV, HSE, NPD) apply a formula of the type $Q_u = k\sqrt{\gamma}\beta$ (where γ is the chord radius to thickness ratio), however, with different values of k . Recently, these formulations have been reviewed /97/ in view of a new experimental and numerical data basis for T and Y joints. While the latter form of Q_u with $k = 4.75$, fits the mean numerical data generated by nonlinear shell analysis, it represents a lower bound on experimental data.

A closer look at the data for axially loaded T/Y joints reveals that the strength factor Q_u is determined from tests with loads in the chord, which makes Q_u smaller than it otherwise would be. However, when using Eq. (5.1) with this Q_u , also a Q_f factor is applied. To avoid that the effect of load in the chord is accounted for twice the initial Q_u should be adjusted to correspond to zero beam-bending /98/.

5.3 Model uncertainty for simple joints

Table 6 summarizes the uncertainty data of the formulations proposed by Yura /92/ and used in existing API guidelines. This table also shows the uncertainties implied by one slightly modified formulae, using a new data basis, which appears to be an improvement. The large scatter experienced for tensile loading is in part due to imprecise formulation of the ultimate limit state. For this reason, it may be necessary to establish two types of limit states for tensile loading, namely one referring to initial crack occurrence and one based on the ultimate load capacity.

Clearly, the uncertainties depend on how the joints are categorized in terms of geometry and load conditions. The wider variety of cases considered in one category, the larger is the scatter. It is also, therefore, necessary for instance, when all joints with in-plane bending are treated together in one category, to ensure that the data basis is representative. But for joints subject to bending there is very limited reliable experimental data for other joints than T/Y-joints, and the uncertainty measures need to be judgementally adjusted.

Table 6 Model Uncertainty of Design Formulae for Unstiff Tubular Joints

Joint type	Load type	Yura/API /92/		Study /96/ ¹⁾		
		B	COV (%)	B	COV (%)	Formu
T & Y	tension	1.41	41	1.06	15	CS
X & DT	tension			1.15	30	DEn/
T & Y	compression	1.07	8	1.11	23	DEn/
X & DT	compression			1.14	12	CS
K & YT	compression	1.17	17	1.34	16	DEn/
All	in-plane-bending ²⁾	1.23	14	0.97	21	CS
All	out-plane-bending	1.09	27	1.17	15	CS

¹⁾ All formulations except the one for X & DT joints and in-plane bending are based on Yura. The model uncertainty is determined by using a data basis.

²⁾ Based on a new numerical data basis, the bias and COV for $Q_u = k\beta\sqrt{\gamma}$, $k = 4.75$, are found /97/ to be 1.02 and 7.8%.

While some qualitative information about the uncertainty of interaction equation is given in /97/ more work is needed to quantify the uncertainty and choice of interaction equations.

5.4 Other joints

In practice, other plane joint configurations than simple T, Y, X, KT and K are applied. For instance, KT joints may have to be classified according to the predominant loading, as shown in Fig. 9b. However, the presence of an unloaded member would necessarily influence the strength to some extent, and, hence, the model uncertainty when the formulae for simple joints are applied.

In connection with multiplanar joints, it is necessary to distinguish between situations where joints in a plane are loaded and hence refer back to the cases discussed, and situations with truly three-dimensional loading. The effect of the 3D-character of the loading is substantial for double K-joints as illustrated in Fig. 9c. Double K-joints are discussed in /89/. Guidance on multiplanar joints is limited but some correction factors for multiplanar effects are given in /86,99,112/, however, with no explicit assessment of uncertainties.

Code provisions for ring stiffened joints are also rather limited. Obviously, it is not practicable to establish parametric expressions for such joints, and one is referred to using calculation procedures.

Clearly, there is a need for systematic experimental/numerical studies, including some benchmark tests, to assess the implied uncertainty of current methods used to determine the strength of complex tubular joints.

6. FATIGUE LIMIT STATES FOR WELDED JOINTS

6.1 General

In the design of marine structures against failure under cyclic loading, high cycle fatigue in welded joints, is of main concern. In general, limit states for fatigue and fracture could most accurately be established by fracture mechanics methods, especially when the effect of inspection is to be taken into account. However, the basis for current design practice both for platforms and ships subject to variable amplitude loading, is still primarily SN curves combined with the hypothesis of linear cumulative damage according to Miner-Palmgren (MP) /16,17,106-110/. Despite the deficiency of the MP method often observed, there is no competitive approach for use in design.

Adopting the SN-MP approach, the limit state may then be written:

$$\sum \frac{n_i}{N_i} - D = 0, \quad N_i = K S_i^{-m} \quad (25a,b)$$

where n_i and N_i are the number of cycles in stress range block (i) and N_i the corresponding number of cycles to failure, K and m are material/geometrical parameters. Possibly different (K,m) sets can be applied for different regimes of S . D is the cumulative damage at failure. The stress (load effect) may either be a nominal member stress, often used for steel plated structures or a hot spot stress, e.g., used for tubular joints in offshore structures.

Fatigue failure in connection with constant amplitude loading is typically defined as visible crack, through thickness crack, or loss of strength of the specimens used. Hence, there is residual fatigue endurance both for tubular joints, and especially for steel-plated structures when the former two types of limits are reached. However, to utilize this residual life under variable amplitude loading, it is necessary to document that premature fracture does not take place due to an overload occurring in the random load history.

6.2 SN curves and stress concentration

The fatigue strength of welded steel joints depends largely upon their geometrical properties: the initial crack size, weld geometry and other geometrical parameters causing stress concentration. The fatigue (crack growth) strength is practically independent of, e.g., yield stress, even if ref. /115/ reports an increase in fatigue life by a factor of 1.5 to 2.0 for cruciform joints made of HT-steel compared to mild steel.

In the nominal stress approach, the SN curve refers to a nominal stress, which includes gross stress

concentration, while the effect of weld geometry etc. is taken into account in the SN curve. In principle, an infinite number of SN curves then need to be considered to represent a variety of welded joints encountered in practice. However, in actual fatigue design codes, nine curves (BS 5400 /102/) and fifteen curves (ECCS /103/, IIW /104/) have been found to be appropriate. BS 5400 has been widely used for offshore codes (e.g., BV /107/, HSE/DEN /16,10/, NPD /17/, DnV-CNF /10) together with an appropriate SN curve for tubular joints. Recently, BS 5400 has been adopted as a basis for ship rules (e.g., ABS /109/, DnV-S /110/). GL /15,111/ uses IIW /104/ (ECCS) supplemented by a classification of many details types for ship structures. API codes are based on ANSI/AWS codes /112/, however, with their own version of SN curves for tubular joints. In the recent revision of US bridge code /113/ the SN curves were adjusted to conform with the ECCS/IIW curves /104/. In the studies /115-116/, an alternative fatigue joint classification for ship details was proposed.

Tubular joints are treated by the hot spot stress concept using one (e.g., DEN/HSE, NPD, ...) or two curves (e.g., BS 5400 C and D) which account for the local weld geometry. The stresses (or stress effects) applied are of nominal member stresses times stress concentration factor which takes into account the overall stress behavior of the tubular joint. The T-curve used for tubular joints by HSE/DEN and NPD/DnV-CNF, is practically identical to the D-curve for steel-plated structures. This curve applies to butt welds. API refers to one SN curve for tubular joints with a smooth weld profile and one with no postweld treatment. Clearly, in the hot spot stress approach, the SCF and SN curves are inexorably linked. The determination of SCF is defined by DEN/HSE, but no explicit procedure is given by API; however, different definitions of hot spot stress is one reason for the difference in SN curves. The hot spot stress approach has been recently also introduced for steel-plated joints in offshore structures (DnV-S). Two basic SN curves - one for a smooth welded joint and one for base material, are applied. The SN curves are taken to be in-between the BS 5400 C and D curves. Stress concentration factors due to gross geometric effects such as eccentricities as well as weld geometry is applied on the SN curves.

While the SN curves in the nominal stress approach are directly based on experimental data, the hot spot stress approach refers to a few SN curves and relies on a calculation of the measured SCF. Hence, it is crucial to calibrate the hot spot stress approach using experimental data for fatigue endurance.

Ref. /117/ describes an interesting correlation of the SN curve based on the hot spot stress approach, to several years of experiences of fatigue cracking or no cracking. The problem encountered in this case is associated with the effect of variability or uncertainty on the results.

The basic SN curves are modified to account for:

- environmental conditions (air, cathodic protection, exposure to free corrosion)
- effect of variable amplitude loading
- thickness effect

The SN curves beyond $N > 10^7$ are commonly modified due to the effect of corrosion and variable amplitude loading. Although, under constant amplitude loading, welded steel joints exhibit a fatigue limit, this is not necessarily the case under variable loading, since cracks initiated by high stresses may subsequently propagate under low stress levels. This may be taken into effect by suitably extending the SN curve beyond the endurance level.

Another aspect of variable amplitude loading is stress interaction, i.e., influence of previous load cycles on subsequent damage. This effect is not accounted for by the Miner-Palmgren approach.

The basic SN-curves in BV-0 /107/, DEn/HSE /16/, and DnV-S /110/ refer to joints in air or with cathodic protection, with a $m=3$ and $m=5$ for $N < 10^7$ and $N > 10^7$, respectively. In case of free corrosion, the fatigue endurance is reduced by a factor of 2 and no reduced slope for $N > 10^7$ is applied. NPD and DnV-CNF use a similar approach, except that for joints with cathodic protection, the curve with $m=3$ applies to $N = 10^8$, at which a fatigue limit is introduced. API /67/ recommends a corrosion limit at $N = 10^7$ or $2 \cdot 10^7$ for the X and X' curves in atmospheric service, while no endurance limit is used for free corrosion. ABS-S /109/ seems to refer only to one set of SN curves.

It is noted that for ships it is normally required that the fatigue analysis is carried out by reducing the nominal plate thicknesses with the corrosion allowance. The thickness effect is generally accounted for by a correction factor $(t_{ref}/t)^{m/4}$ on the fatigue life; however, the reference thickness t_{ref} varies slightly in different codes. The API approach for tubular joints accounts for thickness and weld profile, as explained in /118/.

6.3 Model uncertainties

6.3.1 General

The limit state is described by SN data and the Miner-Palmgren approach. However, since stress concentration factors for nominal stresses are intimately related to the fatigue resistance, uncertainties in SCF's are briefly commented upon.

The BS 5400/DEn/HSE curves are given with uncertainty measures (bias, COV) for K, while m is considered constant (typically equal to $m = 3$). Uncertainty measures of the ANSI/AWS/API data are given in /119/. The uncertainty in the fatigue endurance, N may be modeled by Weibull or lognormal

distributions /120/. While the Weibull model is theoretic preferable, the lognormal model is frequently used.

If the joints are classified according to characteristic fatigue strength, it should be noted that this will imply that each class will include joints with different mean value and standard deviation, if only the characteristic value (mean minus two standard deviations) is the same. This would increase the scatter of the joint category.

The model uncertainty is determined by endurance data in the range of 10^5 to 10^7 cycles, and the uncertainty is representative for this range. Extrapolation, e.g., beyond 10^7 , is obviously uncertain, especially because corrosion, variable amplitude loading and other phenomena affect this of SN-curves. This fact is also implied by the different models used for this area, and should be reflected in a larger model uncertainty for that range.

6.3.2 Stress concentration factors

Fatigue design approaches based on the nominal stress approach, incorporate the effect of weld and other local geometry in the SN curves. Hence, only more "global" geometrical effects need to be accounted for in the stress concentration effect. However, assigning (new) welded joints to one or several categories without using experimentally determined data, would imply a certain (model) uncertainty.

The hot spot approach (used so far for tubular joints on offshore platforms and for ships, e.g., by DnV) is based on one or a few basic SN-curves and carefully determined stress concentration factors. Parametric formulae generated from systematic experiments and finite element analyses, are good for common cases, while otherwise an ad hoc determination of SCF by experimental or numerical methods is required. Table 1 compares model uncertainties for some parametric formulae for SCF's in tubular joints achieved in /121/. It should be noted that the uncertainty varies with the SCF level, indicating that the formulae are not fully optimized. Also, it is noted that most design codes accept the use of different parametric formulae, which obviously will increase the uncertainty implied by the code. No measures of the uncertainty in the SCF's for steel-plated joints in ships /110/ seem to be available.

For the cases when, say, finite element methods are applied to determine the SCF, it is necessary to have a measure for the uncertainty of the calculation procedure. Obviously, this is only possible if the method is clearly specified (e.g., of element, mesh size, extrapolation of stress to hot spot, etc.).

Table 7 Measured to predicted SCF's in tubular T- and Y-joints, based on data given in /121/

Load SCF range	Uncertainty	Method			
		Gibstein	Kuang	Smedley	UCL
Axial load SCF: 3.3 to 13.7 24 specimens	Bias	0.97	0.92	0.85	0.79
	St. dev.	0.22	0.17	0.11	0.13
In-plane b. SCF: 1.1 to 4.9 12(8) specimens	Bias	0.89	0.96	0.81	0.70
	St. dev.	0.19	0.20	0.19	0.14
Out-plane b. SCF: 1.6 to 10.6 25 specimens	Bias	0.98	1.01	0.91	0.81
	St. dev.	0.18	0.25	0.16	0.11

6.3.3 Miner-Palmgren hypothesis of cumulative damage

The uncertainty in using the MP model can be assessed by calculating D_i (Eq. (6.1)) at failure for specimens (i) subject to variable amplitude loading, based on the actual load spectra and SN-curves for the actual joints. The model uncertainty may be determined by the sample statistics of D_i and the assumption that the random uncertainty (V_D) in D is composed of the model uncertainty of the MP approach (V_Δ) and the uncertainty in the constant amplitude (SN) data (V_{SN}), as follows: $V_D^2 = V_\Delta^2 + V_{SN}^2$ /119/. The data summarized in /119/ indicate a mean Δ in the range 0.8 to 1.6 and a COV in the range of 20-30% for each data set. However, most of these data refer to block loading which yields systematically higher damage ratios than random loading and is, hence, not representative for random loading /122,123/. It should be observed that the model uncertainty of the MP approach, is directly linked to how the SN curve is modeled outside the range of available data (say, $>10^7$); and how the number of cycles are counted in broad-band loading. Broad-band loading seems to give low damage ratios at failure /122,123/. However, no explicit measures of the model uncertainty of the Miner Palmgren approach is given in these references.

7. CONCLUSIONS AND RECOMMENDATIONS

Ultimate and fatigue limit states for establishing design equations, and failure functions for reliability analysis have been reviewed, with a focus on limit states for marine structures.

While experimental results traditionally have been used for validating or calibrating analytical limit state formulations, recent developments in numerical methods provide them a useful supplement. Numerical methods agree well with carefully executed experiments and can be efficiently used to systematically study the influence of geometrical and material parameters.

It is (still) customary to estimate the uncertainty associated with limit state equations by assuming that the experiments represent the "truth". However, this is not always the case - uncertainties in the experiments will often add to the estimated model uncertainty and make it conservative.

The adequacy of limit state functions should be assessed by calculating the bias and COV in relation to experimental and numerical data, possibly as a function of slenderness or other relevant parameters. As the bias represents a design correction to the model, it is particularly important to achieve models with a low COV, V_R . The resistance factor is a direct function of V_R , e.g., $\gamma_R \approx \exp[(\alpha_R \beta_T - k_R) V_R]$ where β_T is the importance factor of the resistance, and β_T is the target reliability index (typically in the range 3.2 to 4). While α_R may be relatively small ($\alpha_R \leq 0.4$) for beam-column joints and jackets, it may be 0.7 to 0.8 for steel-plated panels and shells in floating structures.

Several accurate formulations exist for axially loaded stiffened flat panels, with a bias and COV of 1.1 and 1.2. Accurate prediction of stiffener tripping by strength reduction factors, materials type formulations, still remains unsolved. Current formulations for interaction between axial and lateral loads on stiffened panels imply very large uncertainties, and further experimental/numerical studies should be carried out to resolve this problem.

For merchant ships, resistance formulations based on (linear) buckling analysis with a correction for plasticity are still applied in some codes. Such formulations should be replaced by the more modern approaches used for offshore structures. This will yield more rational design, and reduce the likelihood of errors (by limiting the number of formulations used) and in general ease the transfer of technology between these areas.

In the last decade, ultimate strength formulations for stiffened plate girders subject to in-plane bending and torsion have emerged in the civil engineering community. The uncertainty of the most accurate approach corresponds to a bias and COV of 1.0 and 7%, respectively. Such models also have potential use in marine structures, which should be explored.

While adequate ultimate strength formulations are available for cylindrical columns and beam columns, the formulation for the effect of hoop compression on beam-column behavior used in existing codes, should be improved.

It is particularly important to have accurate formulations for stiffened, large diameter cylinders because the uncertainty in load effects for such components is relatively small compared to that of the resistances, and the uncertainty has a significant influence on the partial safety factor for the resistance.

The API codes LFRD, WSD and 2U contain ultimate strength criteria for cylindrical shells subjected to basic and combined loads. Formulations are more empirical fits to data than desirable, and the difference between LFRD and WSD codes is unnecessary. Among other codes, the DnV-CNB and NPD offer advantages, by applying a generalized Merchant-Rankine approach, which facilitates interaction between elastic and plastic failure, and between different load types. However, the model uncertainties in this formulation should be reduced by introducing appropriate knock-down factors.

With regard to unstiffened cylinders, ISO activities aim at harmonizing formulations (API, NPD) for an international offshore fixed steel structures code by the end of 1994. Some venues for improvement of existing formulations for ring stiffened shells are indicated when the ISO harmonization continues. The largest uncertainties for unstiffened/ring stiffened shells are associated with axial tension and hoop compression as well as bending and hoop compression. Improvement in collapse loads for orthogonally stiffened shells with radial, and radial and axial loading, is also desirable. The treatment of tripping failure of stiffeners also has to be resolved. However, it may be necessary to include more detailed information about imperfections and residual stresses and also systematically use nonlinear FEM to reach such a goal for stiffened thin-walled cylindrical shells.

A major step in developing ultimate strength formulations for tubular joints took place when the results of Yura's reassessment of experimental data were introduced in the API codes in the early 1980's. Several other codes: CSA, DnV, DEn/HSE and NPD have since then emerged, proposing different expressions for ultimate strength, with different range of validity. New experimental data and the quality and systematic use of nonlinear finite element analyses make it appropriate to establish a more universal code for the static strength of tubular joints, with a minimum of uncertainty. Besides rectifying some deficiencies in limit states for simple, unstiffened joints, a more explicit evaluation of the uncertainty in the determination of ultimate capacity of complex, stiffened joints is required.

Limit states for fatigue design of marine structures subject to wave loading, are specified in terms of SN curves and the Miner-Palmgren approach. For offshore structures, formulations based on nominal stress are applied for plated

structures, while the hot spot stress method is used for tubular joints, and exceptionally for other components. W. Germanischer Lloyd for a long time has been applying the nominal stress approach for welded joints in ships, the hot spot stress approach has also been adopted in at least one case for ship structures. It is, therefore, desirable to harmonize the approaches for fatigue design. This would imply agreement when nominal and hot spot stress approaches should be used as well as joint classification in the nominal stress approach and data and procedures for calculating SCF's in the hot spot stress approach.

The uncertainties associated with SN curves, to a large extent, relate to geometrical stress concentration. Where explicit uncertainty measures are available for approaches based on the nominal stresses (and typically nine or more joint classes), less information is available for hot spot stress approaches - in which the major uncertainty is transferred to the SCF (which is normally associated with the load effect). It should be noted that the approach based on nominal stress and joint classes, imply an uncertainty associated with selecting weld joint class. SN-curves should, as far as possible, be based on nominal stresses and experimentally justified SN curves. It is necessary to use hot spot stress approaches for new joints, but an estimate of the uncertainties involved should be obtained and used. Due to the limited amount of experimental data and a complex interaction between variable amplitude loading and corrosion effects, the range of 10^7 cycles and beyond, a larger model uncertainty should be assigned to this part of the SN curve.

When using the limit state equations in reliability analyses, an estimated model uncertainty may have to be adjusted to reflect a different level of geometrical imperfections and other parameters in actual structural components compared to that in the specimens or numerical models. Also, model uncertainties for interaction equations need to be carefully implemented.

Hopefully, (all) codes in the future will include commentary which will be useful in future revisions of the codes.

A benchmark study concerned with the ultimate strength of stiffened panels conducted by this committee, demonstrated the implementation of a method for ultimate strength prediction in a computer program, and its use, may lead to errors (departure from the intended procedures).

To reduce such errors, methods and computer codes need to be validated against benchmark tests, e.g., by ISSC. In addition, quality assurance of actual calculation tasks needs to be exercised. Yet, ultimate strength and fatigue estimates will still be affected by such "human factors".

ACKNOWLEDGEMENT

The committee appreciates very much the contribution from Dr. M. K. Chryssanthopoulos and Mr. C. Tolikas to the benchmark study, and Chapters 3.6-3.7, respectively. We also would like to thank Bureau Veritas, Det norske Veritas and Lloyd's Register of Shipping for kindly and actively participating in the benchmark study.

REFERENCES

- /1/ ISO 2394, "General Principles on Reliability for Structures," Int. Standards Organization, First ed., 1973 (Second ed., 1986: Draft, revision 1994).
- /2/ ISSC IV.1, "Report of Committee IV.1 Design Philosophy," Copenhagen, 1988, Wuxi, 1991, St. John's, 1994.
- /3/ Chryssanthopoulos, M.K. et al., "Imperfection Modeling for Buckling Analysis of Stiffened Cylinders," J. Struct. Engng., ASCE, vol. 117, no. 7, July 1991.
- /4/ Ang, A.H.-S., "Structural Risk Analysis and Reliability-Based Design," J. Struct. Div., ASCE, vol. 99, no. ST9, 1973, pp. 1891-1910.
- /5/ Benjamin, J.R. and Cornell, C.A., "Probability, Statistics and Decision for Civil Engineers," McGraw Hill, New York, 1970.
- /6/ Faulkner, D., "Criteria and Guidance for Good Strength Models," Dept. Naval Arch. and Ocean Engng., Report NAOE-91-15, Univ. of Glasgow, July 1991.
- /7/ Moan, T. et al., "Limit States for Tendon and Production Riser Bodies. Selection and Implementation of Limit States as Failure Functions and Design Equations," Report STF70 F93071, SINTEF Trondheim, April 1993.
- /8/ API Bul. 2V, "Bulletin on Design of Flat Plate Structures," American Petroleum Institute, Bulletin 2V, First Edition, May 1, 1987.
- /9/ BS5400, "Code of Practice for Design of Steel Bridges, Part 3" British Standards Institution, London, 1982.
- /10/ BV, "Reglement du Bureau Veritas pour la classification des navieres de longueur superieure a 65m; édition de 1987."
- /11/ DnV-CNB, "Buckling Strength Analysis," Classification Note 30.1, May 1992 (Refer previous version, "Buckling Strength Analysis of Mobile Units," June 1984, revised Oct. 1987)
- /12/ DnV-S, "Rules for Classification of Ships," Det norske Veritas, Oslo, 1992.
- /13/ ECCS, "Recommendations for the Design of Longitudinally Stiffened Webs and of Stiffened Compression Flanges," 1st edition, ECCS Technical Group 8.3 - Structural Stability, Publ. No. 60, European Convention for Constructional Steelwork, 1990.
- /14/ EC3, "Design of Steel Structures, Part 1.1 General Rules and Rules for Buildings," Eurocode 3, 1992, with National Application Documents, Draft for Development, DD ENV 1993-1-1.
- /15/ GL-S, "Rules and Regulations, I - Ship Technology, Part 1 Seagoing Ships, Chapter 1 - Hull Structures," Hamburg, 1992.
- /16/ DEn/HSE, "Offshore Installations: Guidance on Design, Construction and Certification," UK Department of Energy, London, 4th Edition, 1990.
- /17/ NPD, "Regulations for the Structural Design of Fixed Offshore Structures on the Norwegian Continental Shelf," Norwegian Petroleum Directorate, Stavanger, 1993.

- /18/ Dubas, P., Gehri, E. (eds.), "Behaviour and Design of Steel Structures," Publication No. 44, ECCS, Brussels, Jan. 1986.
- /19/ Galambos, T.V. (ed.), "Guide to Stability Design Criteria for Structures," 4th Edition, John Wiley, New York, 1988.
- /20/ Dowling, P.J., Harding, J.E. and Bjorhovde, R. (eds.), "Constructional Steel Design: An Int. Guide," Elsevier Applied Science, London, 1992.
- /21/ Beedle, L.S., "Stability of Metal Structures - A World View," Struct. Stability Research Council (Second Edition), 1991.
- /22/ Rigo, P.H. et al., "Benchmark Study of Ultimate Strength Prediction for Stiffened Panels," to appear.
- /23/ Smith, C.S., Davidson, P.C., Chapman, J.C. and Dowling, P.J., "Strength and Stiffness of Ship's Plating under In-Plane Compression and Tension," Trans. RINA, vol. 130, 1988.
- /24/ Davidson, P.C., Chapman, J.C., Smith, C.S. and Dowling, P.J., "Design of Plate Panels Subject to In-Plane Shear and Bending Compression," Trans. RINA, vol. 132, 1990.
- /25/ Davidson, P.C., Chapman, J.C., Smith, C.S. and Dowling, P.J., "Design of Plate Panels Subject to Biaxial Compression and Lateral Pressure," Trans. RINA, vol. 134, 1992.
- /26/ Smith, C.S., Anderson, N., Chapman, J.C., Davidson, P.C., Dowling, P.J., "Strength of Stiffened Plating under Compression and Lateral Pressure," Trans. RINA, vol. 134, 1992.
- /27/ Chapman, J.C., Smith, C.S., Davidson, P.C. and Dowling, P.J., "Recent Developments in the Design of Stiffened Plate Structures," Proc. of Advances in Marine Structures, Elsevier, Amsterdam, Dunfermline, May 1991, pp. 529-548.
- /28/ Davidson, P.C., "Design of Plate Panels under Biaxial Compression, Shear and Lateral Pressure," Ph.D. Thesis, Imperial College, University of London, 1989.
- /29/ Gordo, J.M. and Guedes Soares, C., "Approximate Load Shortening Curves for Stiffened Plates under Uniaxial Compression," Proc. of Integrity of Offshore Structures, Glasgow, EMAS, London, 1993.
- /30/ Ueda, Y. and Yao, T., "Fundamental Behavior of Plates and Stiffeners with Welding Imperfections," ISMS '91, Shanghai, 1991, pp. 377-388.
- /31/ Bonello, M.A., Chryssanthopoulos, M.K. and Dowling, P.J., "Ultimate Strength Design of Stiffened Plates under Axial Compression and Bending," Marine Structures, vol. 6, no. 5&6, 1993, pp. 533-552.
- /32/ Bonello, M.A., "Reliability Assessment and Design of Stiffened Compression Flanges," Ph.D. Thesis, Imperial College, University of London, 1992.
- /33/ Dowling et al., "Design of Flat Stiffened Plating: Phase 1 Report," CESLIC Report SP 9, Dept. of Civil Engineering, Imperial College, London, Dec. 1991.
- /34/ Vayas, I., "Torsional Rigidity of Open Stiffeners to Compression Flanges," J. Constr. Steel Research, vol. 20, 1991, pp. 65-74.
- /35/ Panagiotopoulos, G.D., "Ultimate Torsional Strength of Flat Stiffeners Attached to Flat Plating under Axial Compression," Marine Structures, vol. 5, 1992, pp. 535-557.
- /36/ Hindi, W.A., "Behaviour and Design of Stiffened Compression Flanges of Steel Box Girder Bridges," Ph.D. Thesis, University of Southampton, January 1991.
- /37/ Ueda, Y., Rashed, S.M.H. and Paik, J.K., "Buckling and Ultimate Strength of Plates and Stiffened Plates under Combined Loads" (published in Marine Structures).
- /38/ Mansour, A.E., "Approximate Formulae for Preliminary Design of Stiffened Plates," Proc. of OMAE '86, Tokyo, 1985.
- /39/ Smith, C.S., "Compressive Strength of Welded Steel Ship Grillages," Trans. RINA, vol. 117, 1975.
- /40/ Rutherford, S.E., "Ultimate Longitudinal Strength of Ships: A Study," SNAME Transactions, vol. 98, 1990, pp. 441-471.
- /41/ Rutherford, S.E., "Stiffened Compression Panels. The Analytical Approach," Technical Report HSR No. 82/26/R2, Lloyd's Register of Shipping, London, 1981.

- /42/ Bonello, M.A. and Chryssanthopoulos, M.K., "Report on Benchmark Test to ISSC Committee V.1" (private communication), 1993.
- /43/ Dowling, P.J. and Harding, J.E., "Box Girders," Chapter 2.7 in /20/.
- /44/ Maquoi, R., "Plate Girders," Chapter 2.6 in /20/.
- /45/ Rockey, K.C., "The Design of Web Plates for Plate and Box Girders - A State of the Art Report," Proc. Int. Symp. Steel Plated Structures," (ed. P.J. Dowling et al.), Imperial College, London, 1976. Crosby Lockwood Staples, London, 1977.
- /46/ Sheer, J. and Pasternak, H., "Zum Nachweis von Vollwandtragern mit dunnen Stegen und Quer-sowie auch Langssteifen in Regelwerken," Bauingenieur, vol. 64, 1989, pp. 121-133.
- /47/ Cooper, P.B., "The Ultimate Bending Moment for Plate Girders," Proceedings of IABSE Colloquim, London, ed. Massonnet et al., IABSE, Zurich, 1972, pp. 291-297.
- /48/ Porter, D.M., Rockey, K.C. and Evans, H.R., "The Collapse Behaviour of Plate Girders Loaded in Shear," The Structural Engineer, vol. 53, no. 8, 1975.
- /49/ Rockey, K.C., Evans, H.R. and Porter, D.M., "A Design Method for Predicting the Collapse Behaviour of Plate Girders," Proc. Instn. Civ. Engrs., Part 2, vol. 65, March 1978, pp. 85-112.
- /50/ AISC, "Load and Resistance Factor Design (LRFD), Specification for Structural Steel Buildings," AISC, Chicago, 1986.
- /51/ BS5950, "The Structural Use of Steelwork in Buildings, Part 3" British Standards Institution, London, 1985.
- /52/ DAST - Richlinie 0.15, "Trager mit Schlanken Stegen," Deutcher Ausschuss für Stahlbau, 1990.
- /53/ "European Recommendations for Steel Construction," EG77-2E, ECCS, March 1978.
- /54/ Jetteur, Ph., Maquoi, R., Massonnet, C. and Skaloud, M., "Calcul des Ames et Semelles Raidies des Ponts en Acier," Construction Metallique (4), 1979, pp. 41-53.
- /55/ Sen, R., "Evaluation of BS5400 Plate Girder Rules," Proc. Instn. Civ. Engrs., Part 2, vol. 81, Sept. 1986, pp. 335-352.
- /56/ Tolikas, C., "Report to ISSC Committee V.1" (private communication).
- /57/ Ostapenko, A., "Shear Strength of Longitudinally Stiffened Plate Girders," Proceedings, Structural Stability Research Council, New York, 1980, pp. 36-40.
- /58/ "Zur Berechnung der Tragfähigkeit augesteifter Vollwandtrager mit schlanken Stegen under Schub-und Biegebeanspruchung in Eurocode 3-Bericht 6057," T.U. Braunschweig, Institut für Stahlbau, July 1988.
- /59/ Narayanan, R. and Der Avanessian, N.G.V., "An Equilibrium Method for Assessing the Strength of Plate Girders with Reinforced Web Openings," Proc. Instn. Civ. Engrs., Part 2, vol. 77, June 1984, pp. 107-137.
- /60/ Narayanan, R. and Darwish, I.Y.S., "Strength of Slender Webs having Non-Central Holes," The Structural Engineer, vol. 63B, no. 3, Sept. 1985, pp. 57-62.
- /61/ Narayanan, R., "Ultimate Shear Capacity of Plate Girders with Openings in Webs," in Plated Structures: Stability and Strength, ed. R. Narayanan, Applied Science Publ., London, 1983.
- /62/ Evans, H.R., "Assessment of Eurocode 3 - Determination of Model Factors for Plate Girders," Report CAR/BRE, Civil Engineering Department, University College, Cardiff, 1985.
- /63/ Evans, H.R., Moussef, S., "Design Aid for Plate Girders," Proc. Instn. Civ. Engrs., Part 2, vol. 85, March 1988, pp. 89-104.
- /63'/ Harding, J.E. and Hobbs, R.E., "The Ultimate Load Behaviour of Box Girder Web Panels," The Structural Engineer, vol. 57B, 1979, pp. 49-54.
- /64/ Singer, J., "Buckling Experiments on Shells - A Review of Recent Developments," Solid Mechanics Archives, vol. 7, 1982, pp. 213-313.
- /65/ Kendrick, S.B., "Structural Design of Submarine Pressure Vessels," Naval Construction Research Est., Dunfermline, Rep. No. R483, March 1964.
- /66/ API (RP2A) WSD, "Recommended Practice for Planning, Designing and Constructing Fixed Offshore Platforms," American Petroleum

- /67/ API (RP2A) LRFD, "Recommended Practice for Planning, Designing and Constructing Fixed Offshore Platforms - Load and Resistance Factor Design," American Petroleum Institute, Washington, First Edition, July 1, 1993.
- /68/ API, Bulletin 2U, "Bulletin on Stability Design of Cylindrical Shells (For use with RP2T)," American Petroleum Institute, Washington, April 1987.
- /69/ "ASME Boiler and Pressure Vessel Code - Nuclear Components," Case N-284, ASME, New York, 1983.
- /70/ BS 5500, "Specification for Unfired Welded Pressure Vessels," British Standards Institute, London, 1976 (Amended April 1981).
- /71/ BS 5950-1, "Structural Use of Steelwork in Buildings, Part 1. Code of Practice for Design in Simple and Continuous Construction of Hot Rolled Sections," British Standards Institution, London, 1990.
- /72/ DnV-OS, "Rules for the Design, Construction and Inspection of Offshore Structures. Appendix C - Steel Structures," Det Norske Veritas, Oslo, 1977 (Revised 1982).
- /73/ ECCS, "European Recommendations for Steel Construction. Section 3. Buckling of Shells," European Convention of Constructive Steelwork, Publication 29, Second Edition, 1983 (ECCS Bull., 1988 Ed., 1988).
- /74/ "Buckling of Offshore Structures," J.P. Kenney and Partners, London, Granada, 1984.
- /75/ Frieze, P.A., "Tubular Member Strength Formulations - International Harmonization," Report OTO/94/102, Health and Safety Executive, London, August 1993.
- /76/ Loh, J.T., "A Unified Design Procedure for Tubular Members," OTC 6310, Offshore Technology Conference, Houston, Texas, May 1993.
- /77/ Miller, C.D. and Saliklis, E.P., "Analysis of Cylindrical Shell Buckling Database and Validation of Design Formulations," API PRAC Paper 90-56, Report, CBI, February 1993.
- /78/ Prion, H.G.L. and Birkemoe, P.C., "Beam-Column Behavior of Fabricated Steel Tubular Members," J. Struct. Engng., ASCE, 118, no. 5, May 1992, pp. 1213-1232.
- /79/ Hellan, Ø., Moan, T. and Drange, S.O., "Use of Nonlinear Pushout Analysis in Ultimate Limit State Design and Integrity Assessment of Jacket Structures," Proc. 7th BOSS Conf., MIT, July 1994.
- /80/ Odland, J., "Buckling of Unstiffened and Stiffened Cylindrical Shell Structures," Norwegian Maritime Research, vol. 1, no. 3, 1978.
- /81/ Cho, S.-R. and Frieze, P.A., "Strength Formulation for Stiffened Cylinders under Combined Axial Loading and Internal Pressure," J. Construct. Steel Research, vol. 9, 1988, pp. 3-31.
- /82/ Moan, T. et al., "Limit States for the Ultimate Strength of Tubular Members Subjected to Pressure, Bending and Tension Loads," J. Struct. Engng., to appear, 1994.
- /83/ Conoco/ABS TLP Rule Case Committee, "Model Code for Structural Design of Tension Leg Platforms," ABS, New York, February 1984.
- /84/ Das, P.K., Faulkner, D. and Guedes da Silva, A., "Limit State Formulations for Reliability-Based Analysis of Orthogonally Stiffened Cylindrical Shell Structural Components," Dept. of Naval Architecture and Ocean Engineering, University of Glasgow, Rep. No. NAOE-91-26, August 1991.
- /85/ Das, P.K., Faulkner, D. and Zimmer, R.A., "Efficient Reliability-Based Design of Ring and Stringer Stiffened Cylinders under Combined Loads," Proc. 6th BOSS Conf, Univ. College, London, 1992.
- /86/ CIDECT, "Design Guide for Circular Hollow Section (CHS) Joints Under Predominantly Static Loading," by J. Wardenier et al., Verlag R. Oldenbourg, Rheinland, GmbH, Köln, 1991.
- /87/ CSA, "Code for the Design Construction and Installation of Offshore Structures," Preliminary Standard S473-M1989, Canadian Standards Association, December 1989.
- /88/ DnV-OFS, "Rules for Classification of Fixed Offshore Installations," Det norske Veritas, Oslo, July 1989.

- /89/ Paul, J.C. et al., "Ultimate Behavior of Multiplanar Double K-joints of Circular Hollow Section Members," Int. J. Offshore and Polar Engng., vol. 3, no. 1, March 1993, pp. 43-50
- /90/ Marshall, P.W., "Design of Welded Tubular Connections: Basis and Use of AWS Code Provisions," Elsevier, Amsterdam, 1992.
- /91/ Wimpey Offshore, "Background to the New Static Strength Guidance for Tubular Joints in Steel Offshore Structures," Report OTH 89 308, Department of Energy, HMSO, London, 1990.
- /92/ Yura et al., "Ultimate Capacity Equations for Tubular Joints," Paper No. OTC 3690, Offshore Technology Conference, Houston, Texas, 1980.
- /93/ Ochi, K. et al., "Basis for Design of Unstiffened Tubular Joints under Axial Brace Loading," Proc. IIW Conf. on Welding of Tubular Structures, Doc. XV-561-84, Boston.
- /94/ Underwater Engineering Group, "Design of Tubular Joints for Offshore Structures," UEG/CIRIA Report UR33, EUG Offshore Research, London, 1985.
- /95/ MSL Engineering, "Static Strength of Tubular Joints on Offshore Structures," Report to Health & Safety Executive, 1992.
- /96/ Ellinas, C.P., Lalani, M. and Sharp, J.V., "Tubular Joint Strength Formulations. The Implications for Harmonisation," Proc. SUT Int. Conf. on API RP 2A-LRFD, Its Present and Future Role in Offshore Safety Cases, London, 24 Nov. 1993.
- /97/ Healey, B.E. and Zettlemyer, N., "In-Plane Bending Strength of Circular Tubular Joints," Proc. Fifth Int. Symp. on Tubular Structures, Nottingham, U.K., August 1993.
- /98/ "Report to ISO TC 67SC7 on Harmonization of Static Strength Standard of Offshore Tubular Joints and Members" (M. Birkinshaw, Convener), 22 March 1993.
- /99/ Paul, J.C., Valik, C.A.C. v/d, Wardenier, J., "The Static Strength of Circular Multi-Planar X-Joints," Proc. Int. Symp. on Tubular Structures, Lappeenranta, Finland, September 1989, Elsevier, 1990.
- /100/ ISSC III.2, "Report of ISSC Committee III.2. Fatigue and Fracture," Copenhagen, 1988; Waxi, 1991; St. John's, 1994.
- /101/ "Fatigue Handbook," A. Almar-Ness (ed.), Tapir publishers, Trondheim, 1985.
- /102/ BSI 5400, "Steel, Concrete and Composite Bridge," Part 10, Code of Practice for Fatigue," British Standards Association, 1980.
- /103/ ECCS, "Recommendation for the Fatigue Design of Steel Structures," Publication No. 43, European Convention for Constructional Steelwork, Brussels, 1985.
- /104/ "Design Recommendations for Cyclic Loaded Welded Steel Structures," Welding in The World, vol. 20, no. 7/8, 1982.
- /105/ "Background to New Fatigue Design Guidance for Steel Welded Joints in Offshore Structures," Department of Energy, HMSO, London, U.K., 1984.
- /106/ DnV-CNF, "Fatigue Strength Analysis for Mobile Offshore Units," Det norske Veritas, Classification Note No. 30.2, August 1984.
- /107/ BV, "Cyclic Fatigue of Nodes and Welded Joints on Offshore Units," Guidance Note N1 199, Bureau Veritas, March 1987.
- /108/ BV-S, "Cyclic Fatigue on Welded Joints on Steel Ships," Guidance Note N1 188, Bureau Veritas, March 1988.
- /109/ ABS-S, "Guide for the Fatigue Strength Assessment of Tankers," A Hull Rule Restatement Project Report, American Bureau of Shipping, NJ, 1992.
- /110/ DnV-CNFS, "Fatigue Assessment of Ship Structures," Report DNVC 93-0432, Det norske Veritas, Oslo, 1993.
- /111/ Fricke, W., "Fatigue Control in Structural Design of Different Ship Types," Proc. Vth Congress IMAM '93, Varna, 1993.
- /112/ "American Welding Society, Structural Welding Code, Steel," ANSI/AWS D1.1-92, AWS, Miami, 1992.
- /113/ AASHTO, "Standard Specification for Highway Bridges," 14th ed., The American Assoc. of State Highway Transp. Officials, Washington, D.C., 1989.
- /114/ Keating, P.B. and Fisher, J.W., "Evaluation of Fatigue Tests and Design Criteria on Welded Details," NCHRP Report 286, National Cooperative Highway Research Program, September 1986.

- /115/ Munse, W.H. et al., "Fatigue Characterization of Fabricated Details for Design," Report SSC-318, Ship Structures Commi Washington, D.C., 1982.
- /116/ Stambaugh, K.A. et al., "Reduction of S-N Curves for Ship Struc Details," Draft Report SR-1336, Ship Structures Commi Washington, D.C., 1992.
- /117/ Yoneya, T. et al., "Hull Cracking of Very Large Ship Structu Proc. Fifth Integrity of Offshore Structures Conf., Universit Glasgow, EMAS Science Publ., London, 1993.
- /118/ Marshall, P.W., "API Provisions for SCF, SN and Size-Pr Effects," Paper No. OTC 7155, Offshore Technology Confer Houston, 1993.
- /119/ Wirsching, P.H., "Probability Based Fatigue Design Criteria Offshore Structures," Final Report, API PRAC Project 81-15, Ja 1983.
- /120/ "Fatigue Reliability: A State of the Art Review. A Four Series," ASCE J. Str. Div., ASCE, vol. 108, no. ST1, January 19
- /121/ Hellier, A.K., Conolly, M.P. and Dover, W.D., "Stress Concentr Factors for Tubular Y and T Joints," Int. J. Fatigue, vol. 12 1, 1990.
- /122/ Tubby, P.J. and Razimjoo, G.R., "Fatigue of Welded Joints Variable Amplitude Loading," G.S.P. 5573/10A/91, April 1991.
- /123/ Gurney, T.R., "Comparative Fatigue Tests on Fillet Welded J under Various Types of Variable Amplitude Loading in Air," OMAE, vol. III-B, ASME, New York, pp. 537-542.